

Summer 2014

Design, Development and Testing of a Balance Board with Variable Torsional Stiffness and Time Delay

Denise Renee Cruise
Purdue University

Follow this and additional works at: https://docs.lib.purdue.edu/open_access_theses



Part of the [Kinesiology Commons](#), and the [Mechanical Engineering Commons](#)

Recommended Citation

Cruise, Denise Renee, "Design, Development and Testing of a Balance Board with Variable Torsional Stiffness and Time Delay" (2014). *Open Access Theses*. 417.
https://docs.lib.purdue.edu/open_access_theses/417

This document has been made available through Purdue e-Pubs, a service of the Purdue University Libraries. Please contact epubs@purdue.edu for additional information.

**PURDUE UNIVERSITY
GRADUATE SCHOOL
Thesis/Dissertation Acceptance**

This is to certify that the thesis/dissertation prepared

By Denise Renee Cruise

Entitled

Design, Development and Testing of a Balance Board with Variable Torsional Stiffness
and Time Delay

For the degree of Master of Science in Engineering

Is approved by the final examining committee:

Arvind Raman

Howard Zelaznik

Shirley Rietdyk

Jeffrey Haddad

Eric Nauman

Justin Seipel

To the best of my knowledge and as understood by the student in the *Thesis/Dissertation Agreement, Publication Delay, and Certification/Disclaimer (Graduate School Form 32)*, this thesis/dissertation adheres to the provisions of Purdue University's "Policy on Integrity in Research" and the use of copyrighted material.

Arvind Raman

Approved by Major Professor(s): _____

Approved by: Dave Anderson

07/25/2014

Head of the Department Graduate Program

Date

DESIGN, DEVELOPMENT AND TESTING OF A BALANCE BOARD WITH
VARIABLE TORSIONAL STIFFNESS AND TIME DELAY

A Thesis

Submitted to the Faculty

of

Purdue University

by

Denise Renee Cruise

In Partial Fulfillment of the

Requirements for the Degree

of

Master of Science in Engineering

August 2014

Purdue University

West Lafayette, Indiana

To my wonderful husband, Dustin, and my always supportive parents.

ACKNOWLEDGEMENTS

When looking back at your accomplishments over time, it is necessary to acknowledge all of the people who have gotten you to where you are today. First and foremost, I would like to thank my parents for always encouraging me to learn as much as possible, try new things, and to never give up. Equally important for me has been having my husband, Dustin, by my side. He is always there for me to lean on, ask advice from, or just talk to after a hard day.

Academically, I would like to thank all of the Professors that I have had the pleasure of knowing while at Purdue University, both in Biomedical Engineering as an undergraduate student, and in Mechanical Engineering as a graduate student. Specifically, I have so much gratitude for my advisor, Arvind Raman. He has never failed to encourage me, help me form new ideas, and acknowledge my work. The postdoctoral fellow in my lab, Jim Chagdes, has been an asset to my work and my success while working towards this degree.

In addition, my committee members from the Department and Health and Kinesiology, Professors Rietdyk, Haddad, and Zelaznik, have consistently provided their support and ideas. They have significantly impacted my Master's work, and I have been lucky to work with them. Thanks to everyone who has helped me on this journey; I am extremely grateful.

TABLE OF CONTENTS

	Page
LIST OF TABLES	vii
LIST OF FIGURES	viii
ABSTRACT	xiii
CHAPTER 1. INTRODUCTION.....	1
1.1 Review of Neuromuscular Balance Control	2
1.1.1 Vestibular System	3
1.1.2 Somatosensory System	3
1.1.3 Visual System	3
1.2 Previous Studies of Posture on Unstable Surfaces	4
1.2.1 Foam Blocks	4
1.2.2 Wobble Boards.....	5
1.2.3 Alternate Balance Boards.....	5
1.3 Mathematical Modeling of Human Posture.....	7
1.3.1 Single-Segment Model	7
1.3.2 Multi-Segment Model	8
1.3.3 Choosing a Model to Use	8
1.4 Mechanisms of Instability	9
1.5 Gap in Current Technology	10
1.6 Contributions of This Thesis	11
CHAPTER 2. DESIGN OF THE SYSTEM.....	13
2.1 Balance Board.....	13
2.1.1 General Requirements	13
2.1.2 Pneumatic Cylinders and Valves.....	15
2.1.3 Linear Position Sensors	16
2.1.4 Control of the Components	16

	Page
2.1.5	Initial Design and Creation 18
2.1.6	Design Changes..... 19
2.1.7	Final Balance Board Design 20
2.2	Safety Platform 20
2.2.1	General Requirements 21
2.2.2	Design Iterations 21
2.2.3	Final System Design 22
2.3	Human Motion Capture 23
2.3.1	Optical Systems 23
2.3.2	Inertial Sensors 24
2.3.3	The Human Motion Capture System 25
CHAPTER 3.	CONTROL, CHARACTERIZATION, AND EVALUATION OF THE SYSTEM..... 32
3.1	Control of the Balance Board 32
3.1.1	Control Using Labview Software 33
3.1.2	Stiffness Coefficient Values..... 34
3.1.3	Time Delay Values 34
3.2	Wireless Sensors..... 35
3.2.1	Writing the Sampling Program 36
3.2.2	Analyzing the Data 37
3.2.3	Validation 38
3.3	Microsoft Kinect..... 41
3.3.1	Depth Data 41
3.3.2	Skeleton Data..... 42
3.3.3	Challenges 43
3.4	Conclusions..... 44
CHAPTER 4.	MEASURING HUMAN RESPONSES 54
4.1	Human Experiments 54
4.2	Observation of Two Mechanisms of Instability 58
4.2.1	Forward/Backward Leaning..... 58

	Page
4.2.2	Limit Cycle Oscillations 59
4.3	Transient Human Response 59
4.3.1	Alternate Testing Procedure..... 60
4.4	Degrees of Freedom..... 60
4.5	Conclusions..... 63
CHAPTER 5.	CONCLUSIONS AND FUTURE WORK 69
5.1	Balance Devices..... 69
5.1.1	Review of the Balance Board System 70
5.1.2	Tactile Response Platform 70
5.1.3	Robotic Balance Platform..... 71
5.2	Human Testing 72
5.2.1	Conclusions from Initial Testing 72
5.2.2	Alternate Populations 75
5.2.3	Additional Goals of Subject Testing 76
5.3	Overall Conclusions..... 76
	LIST OF REFERENCES 81
	APPENDIX. HUMAN TESTING DOCUMENTS..... 85
	VITA 91

LIST OF TABLES

Table	Page
2-1 General Balance Board Parameters.....	18
2-2 Air Cylinder Parameters.....	18

LIST OF FIGURES

Figure	Page
1-1 Traditional passive wobble board which is created by placing a rigid platform on top of a round, central pivot [30].....	12
1-2 Biodex System SD (Left) [31], Neurocom SMART Balance Master (Right) [32].	12
2-1 Method for Producing Desired Overall Board Moment. Cylinder 1 has a net positive moment on the board, while cylinder 2 has a net negative effect. When these are combined, we produce the desired moment on the board.....	26
2-2 First iteration of the balance board design showing the extruded aluminum frame, the upright air cylinders, the pre-made pivot joint, and the plywood platform along the top.	26
2-3 New low-friction pivot; the upper row, left to right, shows the custom-made aluminum housing, the solid bearing, the thrust bearing, and the central rode. The bottom picture shows all the components assembled to create the low friction pivot for the balance board.....	27
2-4 Second iteration balance board design shown with the low-friction pivots put in place within the system.....	28
2-5 New design of balance board with the cylinders placed at an angle to reduce their vertical force on the platform. The frame is made out of extruded aluminum, and the low friction pivots are in place.....	28
2-6 First version of safety platform which utilized a modular design. Each modular component has the same dimensions as the actual balance board.....	29
2-7 Redesigned safety platform loosely based off of the Biodex Balance System™ SD. A permanent perimeter surrounds the board, hand rails are designed for use if needed, and a display is incorporated which will eventually be a touch screen user interface.....	29

Figure	Page
2-8	Final balance board shown along with the surrounding safety platform. A step was incorporated to simplify stepping onto the board, hand rails were manufactured to be adjustable to different heights, and access holes are placed in the base for easy access to hardware. 30
2-9	Schematic of the Microsoft Kinect™ showing the IR emitter and receiver, the color sensor, the tilt motor, and the microphone array [39]. 31
3-1	Model of a person standing upright on a balance board (left); Person standing upright on our balance board (right). 45
3-2	FPGA portion of the code which reads in the values of the input, the linear position sensor, and exports the values of the outputs, the pressure values of each cylinder. 46
3-3	Schematic showing the architecture of how FPGA, cRIO, and Windows Systems work together [40]. 47
3-4	Main Labview program that uses the stiffness coefficients to calculate and control the desired pressure in each cylinder..... 48
3-5	Case loop used in conjunction with memory items to incorporate the haptic feedback time delay. 49
3-6	Raw data from the Vicon© and 3-Space Wireless Sensors during the three flexion-extension movement showing the change in angle between the upper and lower arm. 50
3-7	Filtered and resampled Vicon© data and Wireless Sensor data shown across time during the test..... 50
3-8	Cross correlation of the Vicon© data with the wireless sensor data. 51
3-9	Comparison of Vicon© data and wireless sensor data once the calculated lag is applied to the Vicon© data. 51
3-10	Flexion-extension data from the Vicon© and wireless sensors that was chosen to be used for validation of the wireless sensors..... 52
3-11	Human diagram showing specific joints that are tracked with the Skeletal Tracking program by Kinect™ [41]..... 52

Figure	Page
3-12 Kinect AP position data of each skeletal joint during quiet standing. Both left and right joint positions are captured and shown (left); left and right joint positions were averaged to get one value to represent each joint (right).....	53
4-1 Results from all three participants performing the discrete step stiffness test. One can observe an initial leaning response in all of the participants as stiffness and damping approach minimum values, and high levels of movement as they try to recover their balance. Periods of leaning are highlighted with orange arrows. There is a return to upright stability as the stiffness and damping values approach their maximums.	64
4-2 Results from all three participants performing the variable time delay test. It can be seen that limit cycles tend to occur as the time delay approaches its maximum value, as highlighted by the orange arrows. Most participants are able to avoid the limit cycle behavior at low time delay values.	65
4-3 Results from all three participants performing the linear ramping torsional stiffness test. We see the behavior that we expect with loss of upright stability leading to forward/backward leaning, indicated with orange arrows, when stiffness approaches a minimum.	66
4-4 Sensor data from all three participants during the linear ramping stiffness test. Sensors were placed on the head, chest, pelvis, thigh, shin, and balance board.....	67
4-5 Joint angles calculated with the sensor data from all three participants during the linear ramping stiffness test. This data shows that the three participants each use different balancing strategies.	68
5-1 Discrete step stiffness test results showing the controlled change in stiffness and damping coefficients, as well as the resulting change in board angle over the time length of the test.....	78
5-2 Linear ramping stiffness test results, showing how the participant moved the board as the stiffness coefficient was changed.	79
5-3 Variable time delay test results, showing limit cycle oscillations as time delay is increased past some critical value, and a return to upright stability as time delay is again set to zero.....	80

LIST OF SYMBOLS

F	force created by cylinder
p	pressure
A	cross-sectional area
d	diameter of the air cylinder
M_{board}	overall moment of the balance board
k_{board}	stiffness gain of the balance board
$k_{3,board}$	cubic nonlinear stiffness gain of the balance board
$k_{\tau,board}$	delayed stiffness gain of the balance board
c_{board}	damping gain of the balance board
τ_{board}	haptic feedback time delay of the balance board
ϕ	angle of the balance board
$\dot{\phi}$	angular velocity of the balance board
I_{board}	rotational inertia of the balance board about its COM
$\ddot{\phi}$	angular acceleration of the balance board
M_{person}	the disturbance moment that a person creates on the system
m_{board}	mass of the balance board

h_{board}	height of the COM of the balance board
I_R	rotational inertia of the balance board about its rotation point
mg	weight of the person on the balance board
h	height of the person's COM
K^{cr}	critical stiffness value, equal to mgh

ABSTRACT

Cruise, Denise R. M.S.E., Purdue University, August 2014. Design, Development, and Testing of a Balance Board with Variable Torsional Stiffness and Time Delay. Major Professor: Arvind Raman, School of Mechanical Engineering.

The ability to balance and maintain upright posture can decline for a variety of reasons, such as aging and neuromuscular impairment. As the ability to balance declines, the risk of falling increases. Falls are a major cause of injury, and often lead to a dramatic decline in quality of life. Currently, to alleviate balance deficiencies, people participate in balance training, which most commonly refers to standing on an unstable balance board; the most common boards used are either passive wobble boards, or more advanced commercial systems such as the Biodex System SD® or the Neurocom SMART Balance Master®. Balance training has been shown to improve both static posture and dynamic balance; however, the current methodologies only utilize stiffness and force control.

It has been shown that there are two distinct mechanisms of loss of postural instability: forward/back leaning, arising from insufficient postural stiffness or decreased neuromuscular gain, and limit cycle oscillations, which arise from excessive time delay in the neuromuscular system [1], [2]. We have created a balance board able to elicit both mechanisms of instability, which can

be achieved through two controllable parameters: torsional stiffness and haptic feedback time delay. In addition to building a functional balance board, a safety platform was also fabricated which ensures both user safety and comfort.

After careful calibration of the balance board and the systems used to gather data, initial human testing was performed. Three major tests were completed: discrete step stiffness, linear ramping stiffness, and variable time delay. These tests confirmed that the balance board system is capable of utilizing both mechanisms of instability; both forward/backward leaning and limit cycle oscillations we observed in all participants.

These initial results are promising, and lead directly into a variety of different options for testing on the balance board. The board can be used to test various populations including athletes, older adults, and people with neuromuscular disorders. The ultimate goal of this balance board would be to create a balance score that can be compared among populations, to use the board for training, and to convert this balance board to a robotic platform that creates individualized training plans for users. This novel balance board system has created a large range of possibilities for the future of balance studies and training.

CHAPTER 1. INTRODUCTION

Loss of upright stability is often due to impairments in one or more of the biological systems used to control balance, which leads to negative impacts on a person's life, such as the inability to walk safely, to navigate stairs, or difficulty doing everyday tasks [3]. Every day humans stand upright, maintain balance, and walk without putting much thought into the task; however, the stability of upright posture often declines as people age [4], [5], or if they experience a neuromuscular disorder [6]. In addition, loss of stability can increase the chance of falling, which has been observed in both older adults [7], and in people with neurological diseases [6]. Falls often lead to a loss of mobility, and people often are forced to become dependent on others following a severe fall [7]. It has been shown that in people over 75 years of age, falls account for two-thirds of accidental deaths [8]. Fortunately, research has found that balance training can be effective in improving both static postural sway and dynamic balance, giving us potential to improve balance in those with known deficiencies [9]. This chapter reviews how a person maintains balance and discusses previous experiments performed on human posture, as well as current mathematical models of human posture.

1.1 Review of Neuromuscular Balance Control

The brain uses three major sensory systems to maintain upright stability: the vestibular system, the somatosensory system, and the visual system [3]. These three systems work in conjunction to gather information about the current position of the body in space, to make a comparison between current posture and the desired posture, and to make any necessary corrections. The relative dependence on each of the three systems is based on the goals of the task and the surrounding environment. For example, one study found that in an environment with good lighting, and a firm base of support, healthy individuals will place the following weights on their balance systems: somatosensory (70%), vision (10%), and vestibular (20%) [10].

If one balance system begins to deteriorate, another system may compensate to ensure their balance continues to function at a high level; however, this balance strategy may not function ideally in every situation. Understanding the specifics of all three of these systems and how they work together is crucial to fully understanding how individuals balance and maintain upright stability. In addition, deficiencies in balance should be closely examined to determine which of the three balance systems (or what combination of the three) is primarily responsible for the balance issues—if this can be done, treatment to improve balance can be more specialized, and therefore more effective for the individual [3].

1.1.1 Vestibular System

The vestibular system is responsible for sensing the body's spatial orientation and acceleration; the primary mechanism for this system of balance. Semicircular canals within the inner ear act as angular accelerometers, while the utricular otoliths act as linear accelerometers. These components work together to estimate the body's position and acceleration within space, and then this information is combined with the other major input systems to maintain upright stability [11].

1.1.2 Somatosensory System

The somatosensory system contains a variety of different sensory organs, including those for proprioception and mechanoreception [12]. Proprioception describes the ability to sense the position of one's limbs relative to one another, called static position, and the detection of the rates of movement of these limbs, known as kinesthesia [13]. Mechanoreception is the ability to recognize a variety of stimuli through mechanical pressure or distortion on mechanoreceptors, which are located throughout the entire body.

1.1.3 Visual System

The human eye and the brain work together to capture and process information about a person's surroundings. Studies have shown that if the visual field of a person is weakened, removed, or compromised, the person becomes increasingly worse at maintaining his/her balance. Interestingly, a person has more difficulty maintaining his/her balance when the visual field is unstable than

when a visual field does not exist, as would be the case if the person was blindfolded [14].

1.2 Previous Studies of Posture on Unstable Surfaces

Although studying humans standing on a rigid surface with static conditions gives us an opportunity to learn about how humans maintain upright stability, it is important to also study humans in other, less stable, conditions. In everyday life, we encounter a variety of surfaces and conditions, so it is necessary to understand how humans react to these situations, especially if they cause a person to be placed at his/her limits of stability. In addition to learning about human posture and balance, these alternative surfaces give us the ability to help improve balance through training. Balance boards are commonly used by athletes in training, as well as by those who have decreased stability, such as older adults.

1.2.1 Foam Blocks

It is interesting to examine postural sway on various support surfaces. Standing on a compliant surface, such as a foam block, can reduce stability enough to allow distinction between healthy patients and those with some balance disorder. This is thought to be due to a significant change in the somatosensory feedback from an unstable surface compared to a rigid surface [15]. As a result, standing on foam increases the amplitude of postural sway, regardless of whether the individual's eyes are open [16]. If standing on an unstable surface increases postural sway, it is reasonable to think that studying a

healthy person on foam may give us insight about individuals who have large postural sway even on solid surfaces, due to some balance disorder.

1.2.2 Wobble Boards

There are ways to reduce stability besides standing on a foam surface: a common method is to place a person on a balance board. The simplest type of balance board currently on the market is a wobble board, shown in Figure 1-1.

Because of its availability and relative low cost, wobble boards are often used for training to improve both dynamic balance and static postural sway. One explanation for this enhancement is thought to be due to the improvement of ankle proprioception [9]. An interesting note about wobble boards is that in addition to commonly being used to improve balancing abilities, athletes, especially soccer players, commonly train with them in order to gain ankle strength to prevent injuries [17].

1.2.3 Alternate Balance Boards

In addition to the passive wobble boards that are often used for balance training, there are two notable controllable balance boards that are commonly used which have some feedback component: the Biodex System SD® and the Neurocom SMART Balance Master®. These two systems can be observed in Figure 1-2.

The Biodex System SD® contains a circular platform that moves similarly to a wobble board, but it has integrated software that allows for control of the torsional stiffness of the board. At very high stiffness levels, standing on the board is very similar to standing on a rigid surface, but at low stiffness levels, the

board is able to move freely about the central pivot point, and balancing becomes much more difficult. There is a user-interface screen that is used to inform the users what their task is, as well as give results from the various tests that can be run. During some tests, the interface even gives real time information about how the participant is balancing, giving them the opportunity to improve based on known performance.

The Neurocom SMART Balance Master® also has controllable torsional stiffness, but has an additional component: control of the visual field of the patient. The platform that the individual stands on moves strictly in the anterior-posterior (AP) direction—this allows a clear relationship to be established between external influences and the resulting posture change. The dynamic visual surround is controlled as desired: either in phase with the person's postural sway, out of phase, or independent of the person's movement. This is especially useful when attempting to separate the different components that contribute to the control of human balance.

Several studies have used both of these commercially available systems. Some of these experiments observed the behavior when individuals interacted with the systems, and whether the systems are effective at measuring balance parameters [18], [19]. Other experiments attempted to determine whether training on these devices improves balance and stability [20], [21]. Due to these studies, it has been determined that the systems are effective at measuring balance parameters, although results cannot necessarily be compared directly when measured by different devices; it was also shown that training on balance board

does improve both static posture and dynamic stability [9]. These two systems are important to balance training because they give researchers and clinicians the ability to control specific parameters, which could potentially lead to more effective training procedures based on the individual's abilities and limitations.

1.3 Mathematical Modeling of Human Posture

Even if the primary method for studying human posture is through experiments, mathematical modeling is extremely useful for predictions, and comparison of results. The human body is a complex structure, with hundreds of muscles and bones all working together to control movement. Because of this, mathematical modelling of an upright human is not straightforward, and many forms of models with varying degrees of complexity have been developed by researchers.

1.3.1 Single-Segment Model

Perhaps the simplest way to model the dynamics of an upright human is with the model of a single-link inverted pendulum, with the ankle acting as the pivot about which rotations occur [22], [23]. The dynamics of an inverted pendulum are well understood, and relatively simple, which facilitates the implementation of a controller of the system. As Peterka discusses, although there are models that include the complexities of human posture, simplifying the biomechanics to match the behavioral level of analysis yields excellent insight [22]. This inverted pendulum model has been applied to experimental data of a human standing on a balance board by coupling the 1 degree of freedom (DOF) inverted pendulum model of the person with a 1-DOF inverted pendulum model

of a balance board [1], and neuromuscular control and time delay have been incorporated in the model, improving the similarity between the mathematical model and actual human behavior [24].

1.3.2 Multi-Segment Model

The single-segment model used by Winter as well as Peterka is relatively simple, making it useful for application in control systems [22], [25]; however, researchers have found that postural sway dynamics cannot be fully captured with single inverted pendulum models [26]. Specifically, hip-joint motion cannot be ignored within the model, even for quiet standing, which leads to a multi-element inverted pendulum model [27]. The dynamics of this model are well studied, though significantly more complicated than those of the single inverted pendulum model. This is necessary to analyze both types of models, evaluating both advantages and disadvantages, before we decide which model we will use.

1.3.3 Choosing a Model to Use

Although the multi-segment model is more comprehensive, capturing all of the intricacies of human movement, it is important to consider whether or not the difference between the two models justifies the increased complexity of a multi segment model. If the single-segment inverted pendulum model is able to capture the dynamics of interest during maintenance of upright posture, then it is advantageous to use this more simplistic model. Researchers have found that the simple inverted pendulum model is fully capable of capturing postural sway [22], and that feedback control can be applied successfully within the model [28].

Based on these findings, we have decided to use the more simplified, single-segment inverted pendulum for the mathematical model.

It is essential to note that the single-segment inverted pendulum model is valid only for the maintenance of upright posture. In Chapter Four, we will discuss the applicability of this simplified model to a person approaching, and possibly surpassing, the edge of stability, where the assumptions for this model may break down.

1.4 Mechanisms of Instability

As previously mentioned, researchers have shown that there are two distinct mechanisms of balance instability [2], [24]. The first, and more commonly discussed, leads to a result of forward or backward leaning. This is due to a loss of muscle stiffness, or a decrease in neuromuscular feedback gain. In this type of instability, a person will no longer be able to maintain a vertical, upright position, but they will instead lean in either direction. The other type of mechanism of balance instability is substantially different than a simple leaning motion in one direction. If a person has an increased time-delay in their neuromuscular feedback system, they will encounter a type of instability known as a limit cycle oscillation. In this case, as the person moves away from their ideal vertical position, they attempt to correct, but they overshoot the ideal position, and this continues, leading to an oscillatory motion [2].

The two unique mechanisms of instability, and their behavioral outcomes, will be a focus as we move forward and begin to consider the design of the balance system.

1.5 Gap in Current Technology

Although the current commercial balance boards have been proven to be a useful tool for studying and improving balance in various populations, they only focus on one mechanism of instability: forward or backward leaning [9]. As previously discussed, it has been shown that there is another mechanism of instability: limit cycle oscillations which can arise due to increases in a person's neuromuscular time delay [2], [24]. The neuromuscular time delay is the total time between when the sensory input is received and when the corrective forces are applied. In typical human neural systems, the time delay range varies between 100 and 500 milliseconds, depending on several factors such as age, the sensory system's functionality, the length of the nerve, etc [29]. As people age, or if they experience neuromuscular disorders, their neuromuscular time delay tends to be longer than young, healthy people. Often, this time delay is not incorporated into the human inverted pendulum model, which is a possible explanation for why many researchers focus only on the leaning mechanism of instability [29].

We want to fill the current gap in balance technology, and create a new balance board that is capable of inducing both types of instabilities when a human subject stands on the board. To do this, it is important for the balance board to have two variable, controllable parameters: torsional stiffness and haptic feedback time delay. It has been shown that limit cycle oscillations can be observed in standing posture on a rigid surface in approximately half of people with increased neuromuscular time delay, either due to a neuromuscular disorder,

specifically multiple sclerosis, or due to acute trauma, resulting in a concussion [24]. Our first hypothesis is that if we create a balance board that is able to induce additional time delay via haptic feedback, we will be able to induce limit cycle oscillations even in young, healthy participants. Our second hypothesis is that we could detect a higher rate of limit cycle oscillations when looking at populations with a long neuromuscular time delay, such as those with neuromuscular disorders.

1.6 Contributions of This Thesis

The work described in this thesis has contributed to advancing the state of the art in several ways.

1. The work describes the design and construction of the first known balance board with both variable torsional stiffness and time delay.
2. The torsional stiffness ranges from near rigid to zero and the time delay can be adjusted from 0 to 1000 milliseconds, with a resolution of 10 milliseconds. Thus the novel balance board allows balance research that has not been possible using current balance board technology.
3. Initial test results on human subjects demonstrated both static and dynamic instabilities. These instabilities could be induced in healthy populations due to the ability to control both torsional stiffness and the feedback time delay of the board.
4. Initial results also show potential for successful testing of populations with various balancing abilities.



Figure 1-1: Traditional passive wobble board which is created by placing a rigid platform on top of a round, central pivot [30].



Figure 1-2: Biodex System SD (Left) [31], Neurocom SMART Balance Master (Right) [32].

CHAPTER 2. DESIGN OF THE SYSTEM

This chapter discusses the design and creation of the balance system, which includes the balance board, the surrounding safety platform, and the components used to collect data.

2.1 Balance Board

The balance board is the primary component of the balance system. As was discussed in Chapter 1, there are two unique mechanisms of balance instability, seen in humans via two behavioral patterns: forward/backward leaning and limit cycle oscillations [2]. The Biodex Balance System™ SD and the Neurocom SMART Balance Master® both can induce the first mechanism of instability: the stiffness of the platform can be reduced until the individual leans in one direction. There are no commercial balance boards on the market that incorporate time delay into their system. The objective is to create a balance board that includes both stiffness control and a variable time delay, so that we can detect both types of balance instability mechanisms.

2.1.1 General Requirements

For the balance board, a list of requirements needed to be fulfilled. The first requirement was to allow a variety of user profiles on the board: the board should be adaptable to people of various heights and weights.

Second, the range of rotation of the board should allow ten degrees in each direction. This would provide enough angle movement for a person to become unstable, but not result in tipping the person off of the board.

As mentioned in the introduction of this section, one of the main goals of this balance board was to incorporate both adjustable torsional stiffness and adjustable time delay. To choose the desired ranges of the stiffness values, the board needs to be unstable when torsional stiffness is at a minimum, and to feel like a rigid platform when the stiffness is at a maximum. Implementing a variable time delay was the main component of the balance board that sets it apart from the others on the market. Time delays ranging from 0 milliseconds to 500 milliseconds should be programmable into the device. This range of time delays is relevant because this is the common range of human time delays [29].

Because this board was intended to be used by human subjects, it was also important to consider human factors principles, specifically usability and creating pleasing products. It has been shown in order to have a pleasing product, it needs to elicit positive feelings from its users, such as: security, confidence, pride, excitement, and satisfaction, and it needs to avoid negative feelings such as aggression, frustration, anxiety, and annoyance [33]. To ensure all of these things, a safety platform was fabricated to surround the balance board, which is discussed further in Section 2.2.

The last requirement was the ability to collect data. In order to give us the capability to analyze the motion of the board and the person on the board, it was

necessary to gather both board data, such as the stiffness value and position, as well as participant kinematics.

2.1.2 Pneumatic Cylinders and Valves

The first task was to determine what type of hardware would be used to provide a displacement-dependent force to the balance board. Although a response similar to that of a spring is desired, its stiffness needs to be adjustable. In order to make the system cost-effective with sufficient force generation and stroke length, pneumatic cylinders were chosen as the actuator.

After comparing various brands of air cylinders, the Original Line® Air Cylinders made by Bimba Manufacturing were chosen. These cylinders are fully customizable. Considering the values calculated and displayed in Table 2-2, each cylinder needed to be able to generate at least 925 Newtons (208 pounds) of force, and allow 10.2 centimeters (four inches) of stroke. Equation 2.1 is used to determine the amount of force a cylinder can create:

$$F = p * A = p * \pi * \left(\frac{d^2}{4} \right), \quad (2.1)$$

where F is the force exerted in Newtons (or pounds), p is the gauge pressure applied to the cylinder, and d is the diameter of the bore piston of the cylinder. Knowing that the maximum pressure (the pressure from the airline in the lab) was 690 kilopascals (100 pounds per square inch), the diameter had to be at least 3 centimeters (1.2 inches). Allowing for a factor of safety of 1.7, cylinders with a bore size of 5.1 centimeters (2.0 inches) were chosen to ensure the creation of the maximum desired force.

After choosing the cylinders, the next step was to choose the pneumatic valves that would be used to control air flow to the cylinders. After comparing many options, an electro-pneumatic transducer made by Marsh Bellofram® was chosen. The specific model chosen, Type 3212, acts as a controller by receiving an analog control signal, converting that value to an associated pressure value, and then monitoring and correcting that pressure value. To do this, it contains a twin solenoid valve system, and an integral pressure sensor, with the ability to add an additional external pressure sensor for more precise control.

2.1.3 Linear Position Sensors

In order to use air cylinders as the actuators, the pressure in the cylinders needs to be varied based on the current position of the board. To determine the angular position of the board at any given time, linear displacement sensors were chosen: these devices output an analog signal that corresponds to the change in length of the air cylinder. The linear position sensors are placed in line with the cylinders, so that the sensor directly measures the piston extension from the air cylinder. This sensor output allows the calculation of the board angle in real time.

2.1.4 Control of the Components

To control the system, the CompactRIO (cRIO) Platform made by National Instruments™ was chosen. The cRIO works as an interface between the hardware and the control algorithms written in the software, LABVIEW, also from National Instruments™. The cRIO was chosen because it is reconfigurable, works in real time, and has a variety of interchangeable modules. To control the board, we calculated the desired moment, $M_{board}(t)$, to be generated by the

actuators about the board's pivot as a function of the angular position of the board from the horizontal position, $\phi(t)$:

$$M_{board}(t) = k_{board}\phi(t) + k_{3,board}\phi^3(t) + c_{board}\dot{\phi}(t) + k_{\tau,board}\phi(t - \tau_{board}). \quad (2.2)$$

There are three different stiffness values: k_{board} , $k_{3,board}$, and $k_{\tau,board}$, which correspond to the passive stiffness, the cubic stiffness, and the delayed stiffness, respectively. There is a damping term, c_{board} , which defines the magnitude of the force that is proportional to the angular velocity of the board. τ_{board} represents the haptic feedback time delay. This equation is discussed in more detail in Chapter 3. It is based on prior work in the literature [1], and includes a time delay in the linear stiffness term.

To implement this control, the cRIO module sends a signal into Labview, from the linear position sensors. With this value, the angle of the board is calculated, and used to determine the required overall moment at that specific time and angle. To create that actuating moment, we need to determine the pressure values needed in cylinders one and two. The overall actuating moment for the board is the superposition of the moments created by the two opposing cylinders (Figure 2-1). This type of control was necessary because it was not possible to introduce negative pressure values to the cylinders. Instead, we controlled both cylinders to create the desired overall actuating moment.

Once the actuation pressure in each cylinder is determined, the cRIO board sends an analog signal to the pneumatic valve that corresponds to a

specific pressure. There are both internal and external pressure valves in the system to help ensure that the cylinders are reaching their desired pressures.

2.1.5 Initial Design and Creation

Using all of the previously discussed components, an initial balance board design was created. We wanted to be able to accommodate a variety of user profiles on the board, and the minimum range of rotation that we desired was ten degrees in each direction. Using the general requirements previously discussed, the exact requirements for the board were derived (Table 2-1).

Table 2-1: General Balance Board Parameters.

Board	Value	Units	Value	Units
Weight	4.5	Kg	10	lbs
Length	61	cm	2	ft
Width	61	cm	2	ft
Height (above)	15.2	cm	0.5	ft
Angle (min)	10	Deg		

Using the parameters in Table 2-1, the requirements for the air cylinder actuators were deduced as follows. The worst loading case was determined to be a 136 kilogram (300 lb) participant standing in the center of the board, leaning 10 degrees in one direction. This condition was analyzed, and the necessary maximum stiffness in the springs was calculated, as well as the nominal stiffness.

Table 2-2: Air Cylinder Parameters.

Spring Parameters	Value	Units	Value	Units
Number of springs	2-4	#		
Location from axis	30.5	cm	1	ft
Displacement	5.3	cm	0.174	ft
Stroke	10.76	cm	0.353	ft
Stiffness/Spring (Max)	8881.8	kg/m	5968.31	lb/ft
Stiffness/Spring	888.2	Kg/m	596.83	lb/ft
Force/Spring (Max)	926.6	N	208.33	lbs

From the specific parameters listed in Table 2-2, a board was fabricated that is shown in Figure 2-2. The frame was created with 80-20 extruded aluminum, and the top is a piece of 9.5 mm (3/8") thick plywood. The cylinders are attached with brackets, and the air is travelling through 6.35 mm (1/4") tubing. The top portion of the balance board and the bottom portion were connected with pre-made pivot joints.

2.1.6 Design Changes

After assembling the board, it was obvious that there was a large amount of friction in the system, due to the pivot that we had originally purchased to connect the bottom and top halves of the board. In order to reduce friction as much as possible, we created our own low friction pivots to connect the stationary bottom portion of the structure to the moving board on the top. Each of these pivots was constructed from a custom-made aluminum housing, a solid bearing, two thrust bearings, and a central rod. These components were assembled together to create the overall structure (Figure 2-3).

The balance board was reassembled, and the new pivots were put in place (Figure 2-4). This change helped significantly to reduce the pivot friction. Without any air in the cylinders, the board pivoted with little resistance

Once air filled cylinders, a new problem was observed. The initial board design worked very well for high torsional stiffness values (i.e. high air pressure values); it felt similar to a rigid platform. However, when the air pressure was set to zero in the cylinders, there remained a residual torsional stiffness which allowed one to maintain balance easily. The minimum torsional stiffness due to

both the system design and unexpected friction in the cylinders was higher than we desired. Because this was one of the primary specifications, and we were early in the overall process, we redesigned the balance board to better fit the desired requirements.

2.1.7 Final Balance Board Design

In order to decrease the minimum torsional stiffness of the balance board, we made two changes. First, we wanted to increase the distance between the platform and the pivot. We did this by inserting a piece of 80/20 that is 11.4 cm (4.5") tall between the pivot and the solid board. Second, we felt that we should also decrease the upward force that the cylinders were applying on the board. To do this, we moved the bottom attachment point from the outside perimeter to an internal structure. This put the cylinders at an angle, decreasing the mechanical advantage they had on the board. Once we put these two changes in place, we found that the minimum torsional stiffness was sufficiently low to destabilize upright posture. A CAD model of the final balance board design was created (Figure 2-5).

2.2 Safety Platform

In order to fulfill all of the requirements, we needed to consider human factors: specifically making the product functional, useable, and safe [33]. Because we are creating a device that will put humans in unstable positions, possibly ones that are uncomfortable, we needed to make sure that we designed the system so that the participants are initially as comfortable as possible. One

important component of this was creating a safety platform to surround the balance board.

2.2.1 General Requirements

This safety platform needs to serve a variety of purposes. Because individuals on the board will be approaching their limits of stability, we needed to create a permanent perimeter surrounding the board for a person to step onto in order to step off of the balance board. This perimeter should be wide enough for easy foot placement. The safety platform also needs to have hand rails that a person could use for support if they felt extremely unstable. Looking at commercial platforms, we see that there is often an electronic user interface that gives the participant instructions, allows him/her to control the beginning of the test and gives him/her feedback on his/her performance. To create a comparable balance board system, we could incorporate an electronic user interface. Initially, this will not be possible, but we want to at least create a place holder for that component in the system. Lastly, because we intend to test various populations on the balance board, we may need to move the system to various testing locations. Due to this, the safety platform needs to be fairly mobile—it does not need to be moved daily, but it should be able to be moved if necessary.

2.2.2 Design Iterations

The first idea for a safety platform was to create a modular structure to surround the balance board. The structure would be made up of eight individual components that had dimensions similar to that of the actual balance board.

These components would lock together when in place, but would easily separate, which would make moving them a viable option (Figure 2-6).

This design had several flaws. The first was that it would be very difficult to properly implement hand rails. In addition, although it would be possible to move each piece, moving eight separate pieces along with the balance board would be labor intensive. Not only did the design not meet some of the requirements, it also was overdesigned in some aspects—the solid perimeter around the balance board only needs to be thick enough for someone to put their foot on. This design gives a person two feet in each direction surrounding the balance board, which is not necessary.

From this point, we made a safety platform that was only one structure. We looked at the Biodex Balance System™ SD for inspiration. Based on their design, we created a circular platform that would encapsulate the balance board. We placed an upright support rail along the back of the platform that the hand rails and user face ledge would attach to. We drew this model in CAD (Figure 2-7), and gave it to the fabricator, Purdue Research Machining Services, to be built.

2.2.3 Final System Design

The final design from the fabricator was very similar to the initial CAD model. The permanent static platform to surround the balance board was made in a square shape rather than a circular shape, for easier manufacturing. A step was added to make it easier to get onto the platform. The safety platform was designed so that the balance board is bolted to the inside. There are casters on

the back, so it can be tipped up slightly, and then rolled easily to its new destination. The final balance board system, including the safety platform, has been built (Figure 2-8).

2.3 Human Motion Capture

A major component of the system is the detection of human participant kinematics. With the LabVIEW™ system, we can record data from the balance board components, but we will need a separate system to record the kinematics of the person on the board. The market of human motion capture systems is rapidly expanding in two areas. The first uses sensors placed on the subject; due to advances in microelectromechanical systems (MEMs) technology, these sensors have been able to be miniaturized. The second area is the method of optical tracking, which has been vastly improved due to higher resolution cameras, and improved tracking algorithms.

2.3.1 Optical Systems

The marker based Vicon© motion capture system is a commonly used optical tracking system with high accuracy of detecting position [34]. To operate this system, passive markers are placed on a subject. A set of cameras, at least six, but often up to nine, are set up around the subjects. These cameras output infrared light which is reflected by the passive markers, and then captured by the cameras. Using this method, the exact position of each marker is identified. Although the system is extremely accurate, there are several negative aspects [34]. In addition, occlusion can be an issue if the participant moves in a way to block the reflective marker from the camera. The most obvious drawbacks of the

Vicon© system are that it requires a large space to work properly, and it is difficult to move to a new testing environment [35].

One new optical alternative for the Vicon© system is the Microsoft Kinect™. This system is also able to output three-dimensional anatomical landmark position data. Its function is possible by emitting infrared (IR) light, and then using an IR depth sensor in conjunction with a color sensor to pick up the signals (Figure 2-9).

The Microsoft Kinect™ is low cost, and has been shown to be comparable to the Vicon© system when analyzing kinematic strategies of postural control [36]. It is also capable of recording standard video footage, which would be very useful for reviewing experiments.

2.3.2 Inertial Sensors

One alternative to the optical methods is the approach of putting the sensor directly on the subject. Inertial measurement units (IMUs) are electronic components that gather information about the subject's velocity, orientation and acceleration. Studies have been completed that show that these IMUs are capable of gathering similar information as the Vicon© system, giving researchers an inexpensive alternative to a full Vicon© camera setup [35]. There are some limitations of IMUs used for absolute position, which are mostly concerned with drift—these errors can be reduced with proper filtering, but can eventually lead the system to be somewhat unreliable when trying to output 3D position data [37]. However, these sensors are generally accurate for orientation values, and relative measurements between various IMUs. There have been

studies to address the problem of IMUs outputting only relative data, rather than specific location data [38].

2.3.3 The Human Motion Capture System

Considering our system's requirements, we purchased two systems to observe and record participant kinematics: Microsoft Windows Kinect™ and several IMU units called 3 Space Wireless Sensors, manufactured by YEI Technology©.

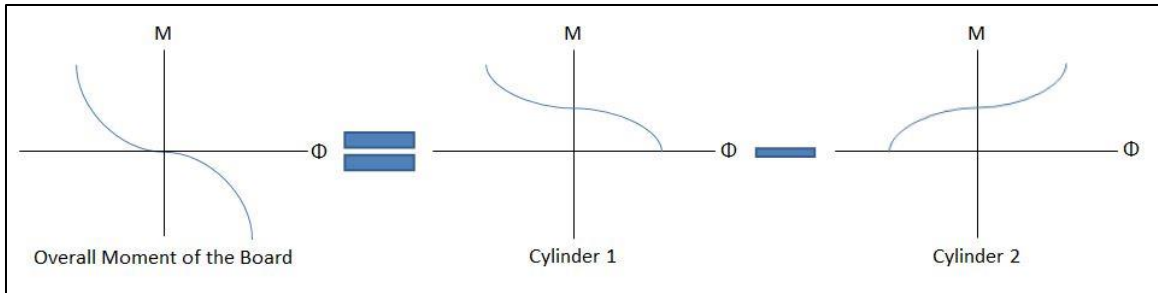


Figure 2-1: Method for Producing Desired Overall Board Moment. Cylinder 1 has a net positive moment on the board, while cylinder 2 has a net negative effect. When these are combined, we produce the desired moment on the board.

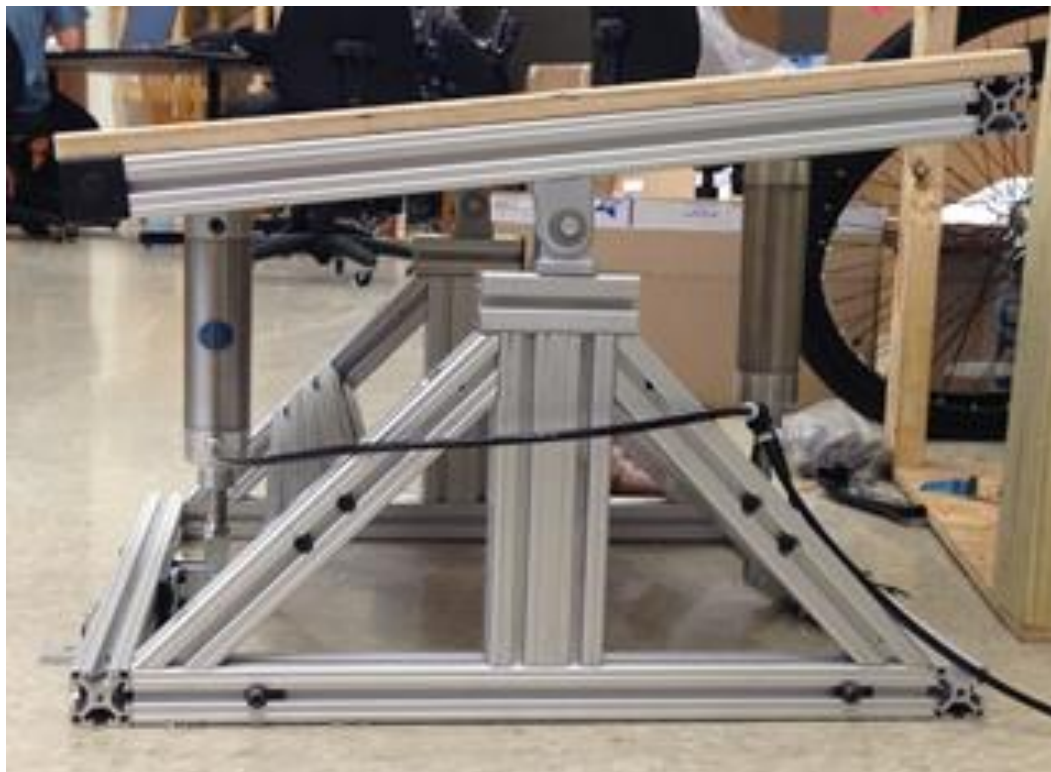


Figure 2-2: First iteration of the balance board design showing the extruded aluminum frame, the upright air cylinders, the pre-made pivot joint, and the plywood platform along the top.

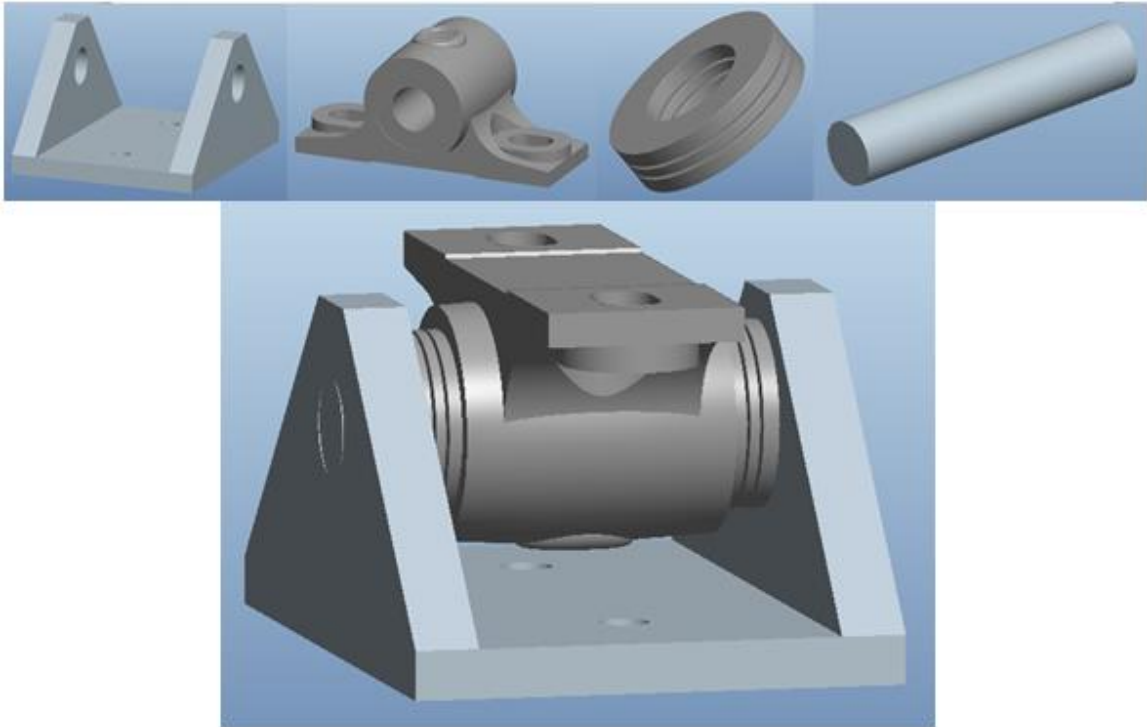


Figure 2-3: New low-friction pivot; the upper row, left to right, shows the custom-made aluminum housing, the solid bearing, the thrust bearing, and the central rod. The bottom picture shows all the components assembled to create the low friction pivot for the balance board.



Figure 2-4: Second iteration balance board design shown with the low-friction pivots put in place within the system.

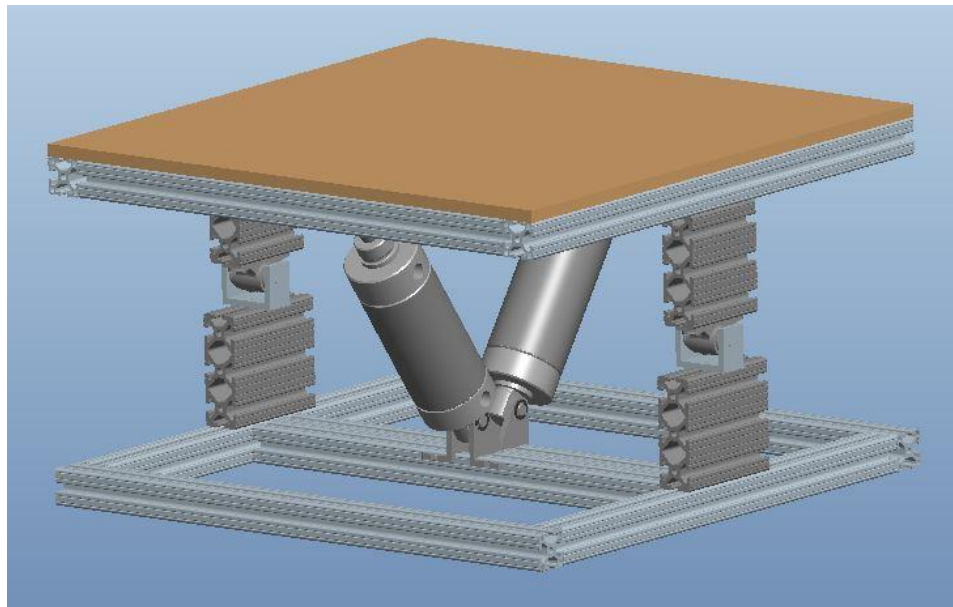


Figure 2-5: New design of balance board with the cylinders placed at an angle to reduce their vertical force on the platform. The frame is made out of extruded aluminum, and the low friction pivots are in place.

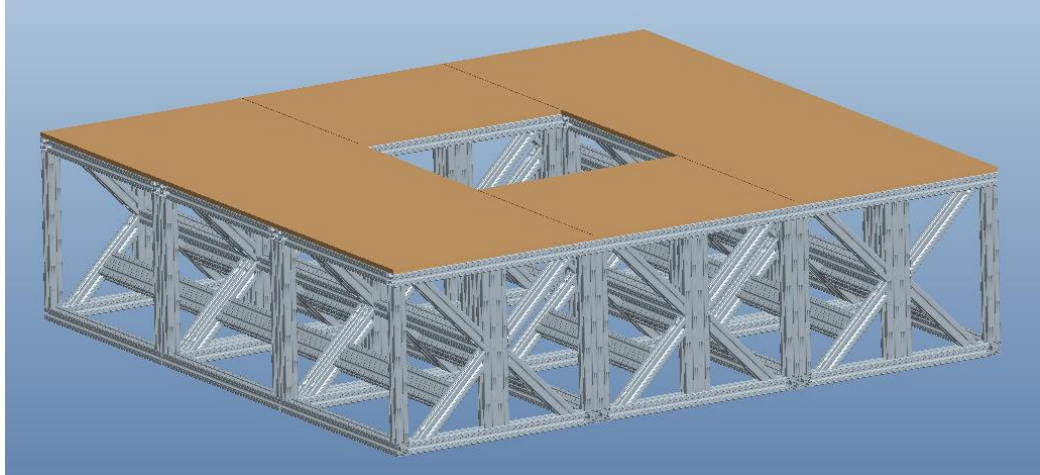


Figure 2-6: First version of safety platform which utilized a modular design. Each modular component has the same dimensions as the actual balance board.

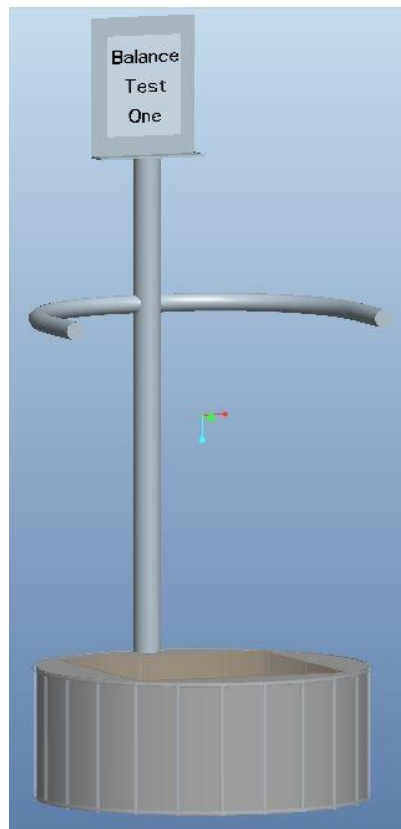


Figure 2-7: Redesigned safety platform loosely based off of the Biodex Balance System™ SD. A permanent perimeter surrounds the board, hand rails are designed for use if needed, and a display is incorporated which will eventually be a touch screen user interface.



Figure 2-8: Final balance board shown along with the surrounding safety platform. A step was incorporated to simplify stepping onto the board, hand rails were manufactured to be adjustable to different heights, and access holes are placed in the base for easy access to hardware.

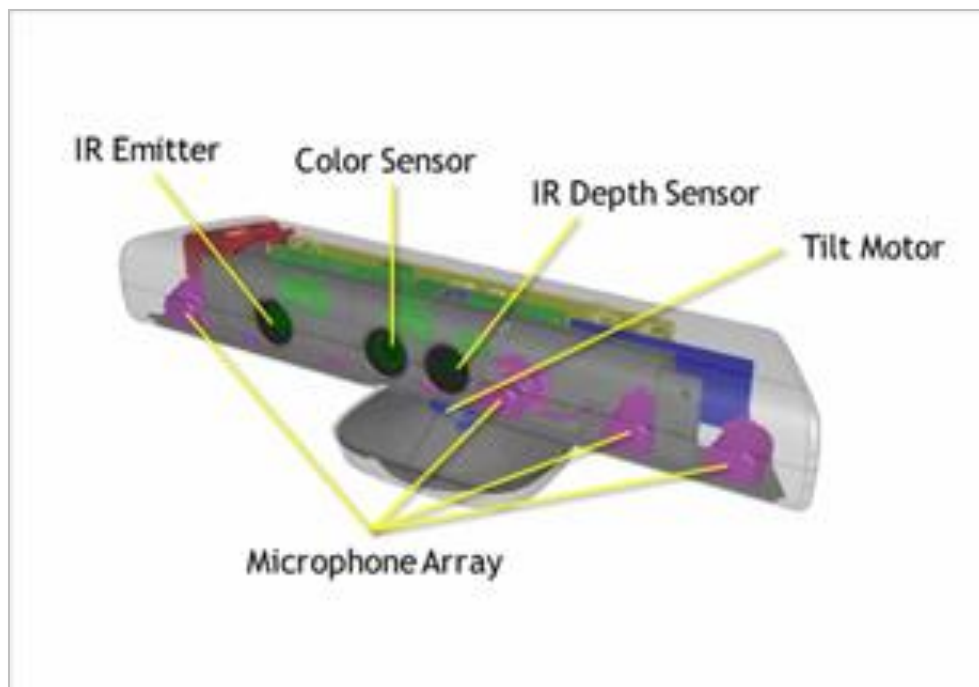


Figure 2-9: Schematic of the Microsoft Kinect™ showing the IR emitter and receiver, the color sensor, the tilt motor, and the microphone array [39].

CHAPTER 3. CONTROL, CHARACTERIZATION, AND EVALUATION OF THE SYSTEM

This chapter will discuss the control and characterization of the balance board, the calibration of the wireless inertial sensors, and the evaluation of the Kinect™ for human motion capture.

3.1 Control of the Balance Board

The first step in designing a controller for a dynamic system is to consider the mathematical model of the system. We model the balance system as a coupled system consisting of two inverted pendulums: the first inverted pendulum is the person as a rigid body with a pivot at the ankle, and the other inverted pendulum is the balance board, with its natural pivot shown in Figure 3-1.

To determine the equation for M_{board} , which will dictate the controller, we chose to have a second-order response, with multiple stiffness terms that represent different conditions:

$$M_{board}(t) = k_{board}\phi(t) + k_{3,board}\phi^3(t) + c_{board}\dot{\phi}(t) + k_{\tau,board}\phi(t - \tau_{board}). \quad (3.1)$$

This fits into the system dynamics as shown in equation 3.2, which is determined by calculating the sum of moments about the pivot of the board:

$$\sum M_{/board_pivot} = I_{board}\ddot{\phi} = -M_{board} + M_{person} + m_{board}gh_{board}\sin\phi. \quad (3.2)$$

In the following sections, we will discuss the terms in Equation 3.1, the contribution of each term to the overall equation, and how we chose specific values to use for the coefficients of the terms.

3.1.1 Control Using Labview Software

The cRIO system contains a field programmable gate array (FPGA), which is an integrated circuit that allows the user to communicate with external hardware very quickly. The program that runs the FPGA is written separately from the program which calculates the pressure values; the FPGA program, seen in Figure 3-2 is very short, and only contains the necessary inputs and outputs within a while loop, so that it runs continuously until the stop button is pressed.

The main portion of the LABVIEW™ code, called the host program, calls the FPGA code, reads in values, uses the values to calculate the desired pressure in each cylinder, and then sends that pressure value back to the FPGA. It is important to remember that this code is not programmed onto the FPGA, but instead it runs on the computer's hard drive, making it easy to save values to a file, reduces compilation times, and removes concerns about storage limitations. A schematic showing how the FPGA, cRIO, and host computer interact is shown in Figure 3-3.

The Labview block diagram can be seen in Figure 3-4. There is a time delay built into the code, but this is not to induce a time delay in the feedback of the balance board, this is to control the timing of the loop. This timing implementation makes the structure deterministic.

3.1.2 Stiffness Coefficient Values

The range of stiffness and damping coefficients were decided upon through trial and error based on the pressure range we had available. After the range of stiffness and damping coefficients had been experimentally determined, these values were normalized so that they could be compared between different people. Normalization was chosen to be with respect to mgh , which is defined as the critical stiffness, K^{cr} , where m is the mass of the person, g is gravity, and h is the height of the center of mass. This normalization is chosen with respect to the model. The values for normalization were determined through a combination of analyzing modeling and simulation results, and through pilot testing. It was decided that the maximum stiffness value for a participant would be $5 * K^{cr}$. The damping coefficient was set to 20% of the K^{cr} value, and the cubic stiffness coefficient was set to 5% of the K^{cr} value. Based on pilot testing, these values led to expected participant behaviors; this gives us a good indication that the modeling and simulations were accurate.

3.1.3 Time Delay Values

Research shows that a healthy person's neuromuscular time delay is between 100-500 milliseconds. A person with a neuromuscular disorder can have a time delay much higher than these standard values [29]. Based on the magnitude of these values, a minimum resolution of 50 milliseconds was chosen for the haptic feedback time delay in the balance board. A wide range of desired time delay values should be able to be incorporated: for example, time delay

should be able to be set to 50 milliseconds, but the system should also be able to function properly with a time delay of 2 seconds.

This variable delay functionality was possible using the LABVIEW™ software. Once the code was written to control the stiffness of the board, the program was modified by adding a time delay component. To do so, the time passed is compared to the desired time delay. If the time passed is not greater than the desired time delay, the code continues to only control stiffness; however, if the loop time is greater than the set time delay, the code enters a different loop. In this case, it calculates the moment in each cylinder with the same equation, except instead of using the current angle, angle value from the value of the time delay in the past is used. This allows the person to feel the delayed feedback from the air cylinders. The application of the feedback time delay is accomplished with a case structure in the LABVIEW™ software (Figure 3-5).

This code worked as expected, which was tested by implementing a set time delay, and then using the software to measure the amount of time it took for one loop to complete. The loop time was consistently two milliseconds longer than the time delay, so another time monitor was added to determine the loop processing time. As expected, it was determined that the loop took two milliseconds to complete, which confirms that the total time recorded was the inputted time delay plus the loop iteration time.

3.2 Wireless Sensors

The 3-Space Wireless Sensors created by YEI Technology, are inertial measurement units (IMU), made with a triaxial gyroscope, accelerometer, and

compass sensor. In addition to the hardware used, there is on-board advanced processing. For outputting orientation values, the sensors implement quaternion-based Kalman filtering algorithms to determine the real-time orientation relative to some absolute reference.

3.2.1 Writing the Sampling Program

YEI Technology has provided some initial sample codes, in both C and Python, to help users get started with the 3-Space Sensors. Python was used for coding, so we started with their initial code for one wireless sensor and continued development for our application. The library that YEI Technology had created for use with the wireless sensors was utilized, and the main portion of the code was written to constantly stream data from the sensors, in order from sensor zero to sensor five. Initially, there was an issue that if one sensor did not successfully send its data to the computer, the code would crash, but this was fixed by writing the bytes to serial rather than streaming them directly to a command window. A header was created that contained key information, such as current time and sensor value, and then the actual data was attached to the header. One downfall of this method is that it does not result in an exact sampling rate, but it does return a time stamp with each data point, so it can be analyzed properly. This is one component of the program that we hope to improve in the future, because having deterministic systems is incredibly useful for signal processing and data analysis.

3.2.2 Analyzing the Data

The 3-Space Wireless Sensors are ideal for outputting the orientation of the device, but they have the ability to output a variety of values, in either raw or filtered form: acceleration, angular velocity, and compass heading. For the purpose of determining angles between various body parts, the orientation of the sensor is appropriate. The sensor can output the orientation value in the form of quaternions, Euler angles, axis angle, rotation matrix, or two vectors (forward and downward). Initially quaternions were decided upon because this form of vector does not have any issues with gimbal lock, but issues were encountered with this method due to quaternions being difficult to visualize. Next, we attempted to look at the orientation in terms of Euler Angles. This worked well if the sensor was placed horizontally, like the one placed on the balance board; however, the sensors on the body were placed vertically, and in this position, the sensors experienced gimbal lock. We observed that two of the Euler angles would be valid, but one would simply give an output of zero when it was indeterminate due to gimbal lock. Finally, the orientation was outputted in the form of two vectors: the forward vector and the downward vector. These vectors are returned in x, y, z components within the global coordinate space.

Once the two vectors that represent the orientation of each sensor were defined, we had to determine how we would use this data to capture the human kinematics. For this, the time series data of the orientation of each sensor was used to calculate the change of angle from the beginning of the data set to the

end. If this was done for each sensor, corresponding to each body segment, the entire body's movement could be visualized.

The first step in analyzing the data is to determine how much the sensor is rotated in the horizontal plane compared to the global coordinate system. The assumption that the vertical component, the y-value, is the same between the sensor coordinate system and the global system is reasonable, but it is necessary to know the difference between the x-z plane. This is step is necessary because we are only concerned with 1 degree of freedom, so it is necessary to make sure the coordinates that the plane corresponds to are known. Once this angle is determined through basic geometry, the difference in angle between the vectors can be calculated using the dot product, shown in Equation 3.3,

$$\vec{a} \cdot \vec{b} = |\vec{a}| |\vec{b}| \cos \theta. \quad (3.3)$$

This method outputs the change in the angle of each sensor, which represents the change in the angle of each segment of the body which the sensor corresponds to. Having this information allows analysis of the movement of each body segment, and lets us determine how the person on the board is moving in relation to the balance board.

3.2.3 Validation

In order to validate the 3-Space Sensors, a comparison was done against a commonly used system for human motion capture, the Vicon© Motion Capture System. To do this test, one wireless sensor was placed on the back of the forearm and one wireless sensor placed on the back of the upper arm. Then

three Vicon© markers were positioned on each sensor, so that the full 3D movement was captured with the array of cameras. The actual experiment involved extension and then flexion of the elbow three times consecutively.

The Vicon© returns the position of each of the six markers. These three position values from each cluster can be used to calculate a “forward” vector that would correspond directly to the forward vector outputted by the wireless sensors. Then the dot product can be used to determine the angle between the two forward vectors created by the Vicon©, and the two forward vectors of the wireless sensors; this is the angle of the elbow at any given time. This elbow angle data is the raw change of angle between the two limbs, as captured by the wireless sensors, and by the Vicon© data; in Figure 3-6 we see this comparison.

Looking at the Vicon© data in Figure 3-6, some high frequency noise is seen, especially in the peaks of each curve. To remove this noise, a low pass filter with a cutoff of 10 Hertz was applied. The other initial processing performed was to resample the wireless sensor data to be at 120 Hertz, the sampled rate of the Vicon© data. This manipulated Vicon© data is shown alongside the sensor data in Figure 3-7.

From this point, the cross correlation was calculated to determine how much lag to apply for the signals to appropriately line up. This lag was a result of two different researchers starting the recording from each system independently. In Figure 3-8, the results of the cross-correlation can be seen; it was determined that the maximum cross correlation is at a value of 164 frames. This indicates that the Vicon© data is 164 samples behind the wireless sensor data.

To properly line up the Vicon© data and the Wireless Sensor data, the calculated lag of 164 samples was applied to the Vicon© signal. Once this lag was applied, the two signals were replotted to determine if there was an improvement in their alignment (Figure 3-9).

As can be seen in Figure 3-9, once the signals had been appropriately resampled, filtered, and lined up in time, they are very similar to one another. After examination, it was determined that the Vicon© data from the first flexion/extension movement was non-standard, and it seemed to show some small error, likely due to an occlusion of one or more of the Vicon© markers during that first movement. Due to this, the first flexion/extension movement was removed from the remaining steps for validation of the wireless sensors. Figure 3-10 shows the Vicon© and wireless sensor data used for the validation of the 3-Space Wireless Sensors.

Once the remaining data had been filtered, resampled, lagged, and windowed, the root mean squared (RMS) value of the wireless sensor data was calculated. The RMS is a statistical value that represents the magnitude of a varying quality, so it seems appropriate to quantify the difference between the wireless sensor data and the Vicon© data. To do this, Equation 3.4 was applied to the data set. The dynamic RMS of the data was found to be 2.06 degrees, calculated as shown:

$$RMS = \sqrt{\frac{1}{N} \sum_{i=1}^N e_i^2}. \quad (3.4)$$

3.3 Microsoft Kinect

The Microsoft Kinect™ was originally created specifically for the XBOX 360™, a video game platform. When programmers started to realize the vast possibilities of the system, Microsoft® released a version of the Kinect™ made specifically for Windows®. This version was released with a Software Developer Toolkit (SDK), which provided some starter code for a variety of applications. One of the programs directly aligned with our goals is the skeletal tracking package, which identifies and tracks twenty joints within the human body. Programs for the Kinect™ can be written in a variety of languages: C#, C++, or Visual Basic, so it is possible to customize an existing program, or to write your own program from scratch.

3.3.1 Depth Data

Because the Kinect™ has a normal color camera, along with an IR emitter and an IR depth sensor, it can reconstruct a three-dimensional image of its field of view. This reconstruction capability also gives it the ability to output the depth of each pixel within the image, in millimeters. This is extremely useful, and a major factor that sets the Kinect™ apart from a normal video camera.

After viewing examples in the Windows SDK, it was decided that we would write a custom program to export the depth of each pixel, using C#. It was necessary to learn how to structure commands within C# architecture, and eventually the desired result was outputted. A colored reconstruction of the image was created where the color of each pixel depended on the how far away that pixel was from the camera. Although learning how to control the hardware

through the software was good practice for future programming tasks, after considering our needs for this project, it was decided that we would be able to use one of the pre-generated programs included in the SDK.

3.3.2 Skeleton Data

For the Skeletal Tracking feature to work properly, the person needs to standing between 0.79 meters (2.6 feet) and 4 meters (13.1 feet) away from the Kinect. The software uses the depth of each pixel to identify where the person is standing, and then uses a variety of algorithms to determine the specific location of the desired joints. The Kinect™ identifies twenty joints using the skeletal tracking feature (Figure 3-11).

Using a program called Kinect Explorer – WPF, which is included in the SDK, the location, in millimeters, of each of the joints can be exported. The location given is in terms of a 3D coordinate system, with the Kinect™ as the origin, the z-axis in the direction that the Kinect™ is facing, and the y-axis pointing upwards (opposite gravity), with a right-handed coordinate system. In addition to exporting the location coordinates, each joint is also given a confidence value: “tracked” means that the joint is clearly visible via the Kinect™, “inferred” indicates that a joint was not clearly visible, and its position is estimated, and “non-tracked” means that no coordinates are given. This “non-tracked” condition may occur if several limbs are not properly detected, for example if someone is seated rather than standing.

Previous research has shown that the Microsoft Kinect™ is accurate enough to assess the human kinematics involved in postural control [36]. Based

on this work, we used the Microsoft Kinect™ for some initial testing of standing posture. A graph showing the results of the joint tracking was created; on the left we see the movement in the anterior-posterior (AP) plane of all of the tracked joints, and on the right we averaged the left and right to get a center average movement of each joint. Note that center of mass is also plotted in the right, lower portion the figure (Figure 3-12). This is a center of mass that was calculated using the joint data. The Kinect™ does calculate center of mass data, but we found that it was generally very noisy; calculating the center of mass at the end of the process using the joint position data showed an improvement in quality.

Based on overall positive results, we chose to use the Microsoft Kinect™ with the Skeletal Tracking feature as a supplementary method to assess human kinematics while participants are on the balance board.

3.3.3 Challenges

The Microsoft Kinect™ samples at a maximum of 30 Hertz. While this is generally fast enough to capture human motion, the Vicon© camera system samples at 120 Hertz, so one concern was that we would not be able to capture all human movement, especially when people approached their limit of stability. Although this was an initial concern, 10 Hertz covers almost the entire bandwidth of postural sway [28] which results in a Nyquist frequency of 21 Hz. As long as we can capture at 21 Hz, we could capture all desired movement. We proceeded with using the Microsoft Kinect™, with the additional advantages of being cost-effective, easy to use, and easy to obtain.

The second, and more crucial, challenge that was faced with the Kinect™ was that the skeletal tracking feature is intended to be calculated by viewing the front of a person. Because of a central pole that is a part of the safety platform that surrounds the balance board, the Kinect™ cannot be placed directly in front of the person/system without an obstruction of view. We plan to place the Kinect™ behind the person to record their movement, but because the skeletal tracking was not created for this purpose, we will not be able to put much confidence in the output of the values.

3.4 Conclusions

We were able to successfully validate and characterize the various components of the balance board system. The range of stiffness and damping coefficients that will be used to program the balance board were determined, and the dynamics of the board were fully analyzed. The wireless sensors have been validated against the Vicon®, and although there is some small level of error, we believe we will be able to capture the vast majority of movement with these sensors. Lastly, the Kinect™ has been tested, analyzed, and will be used for video tracking. Although we plan to utilize the Kinect, we cannot put a high level of confidence in the skeletal data due to nonstandard placement of the Kinect™ in relation to the participant.

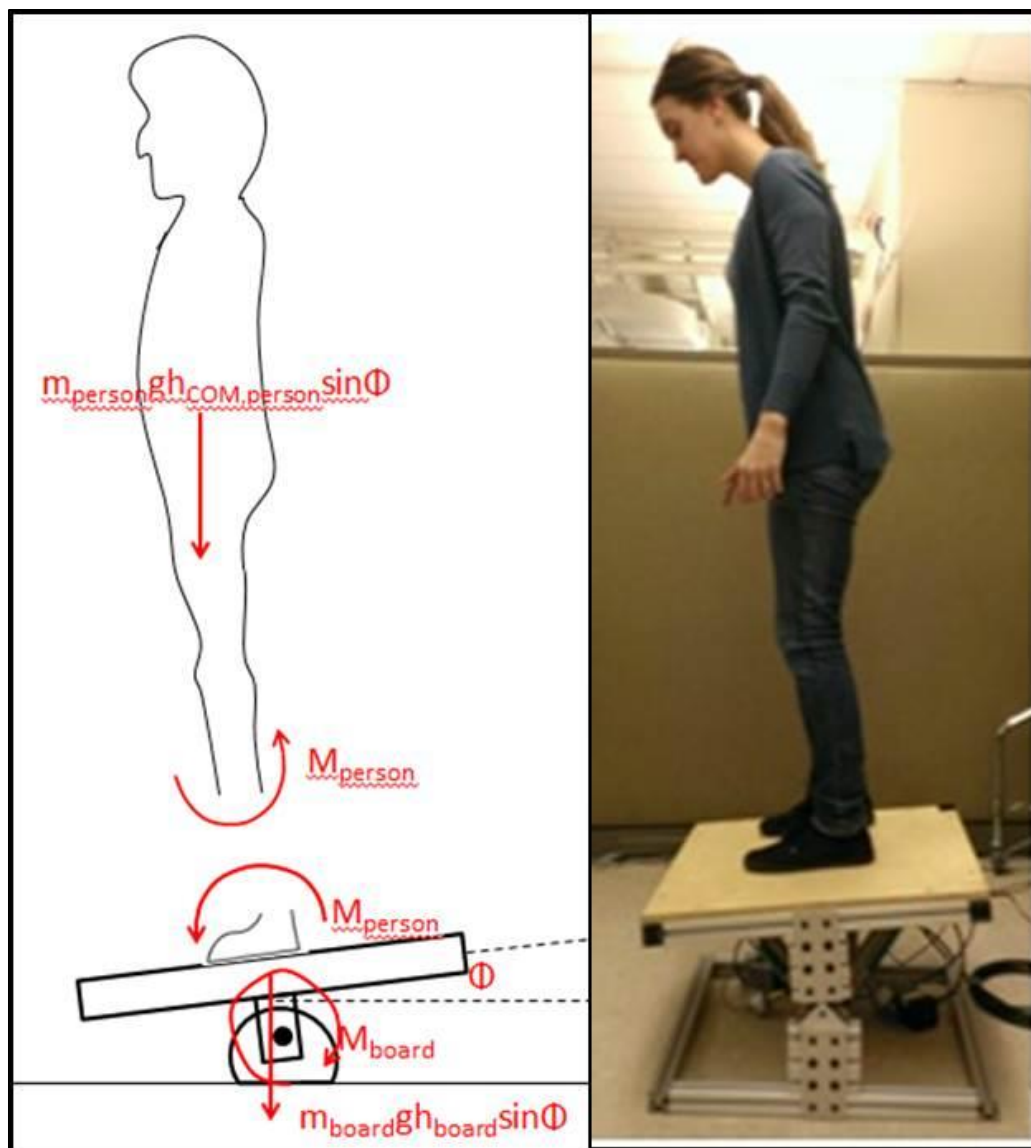


Figure 3-1: Model of a person standing upright on a balance board (left); Person standing upright on our balance board (right).

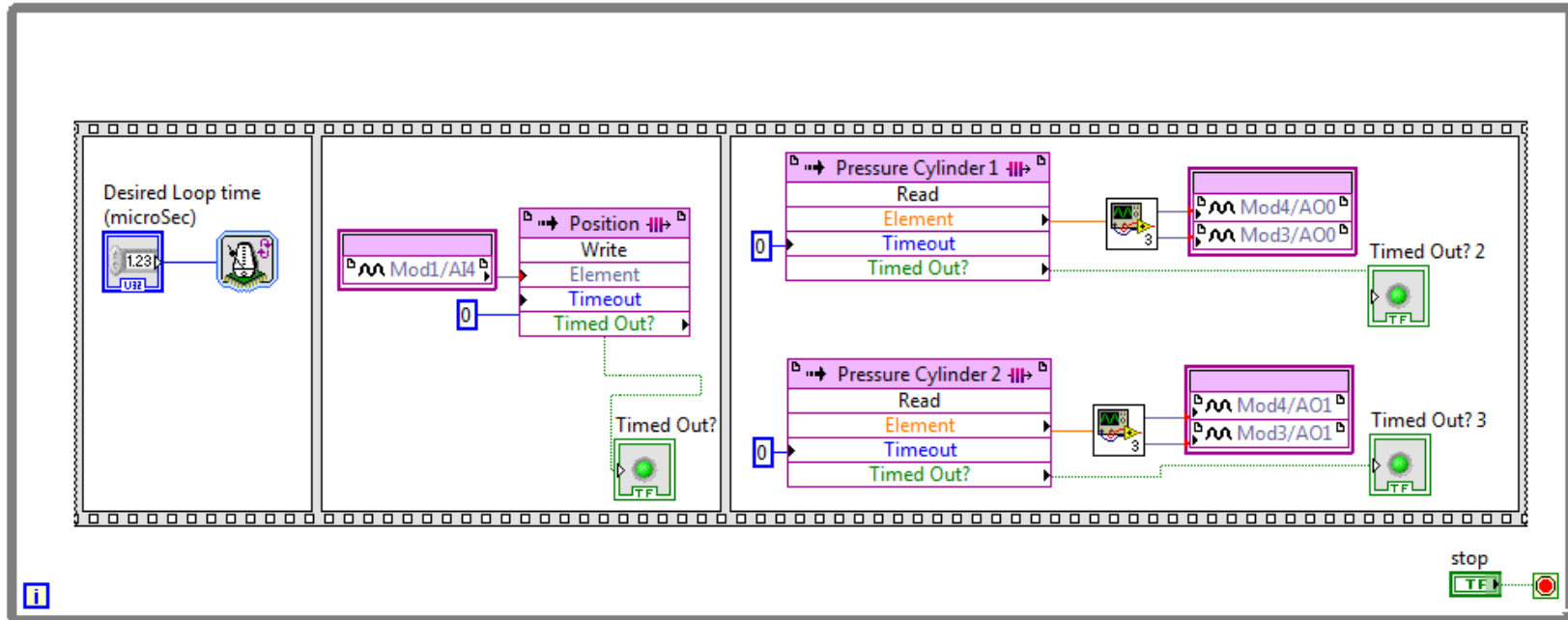


Figure 3-2: FPGA portion of the code which reads in the values of the input, the linear position sensor, and exports the values of the outputs, the pressure values of each cylinder.

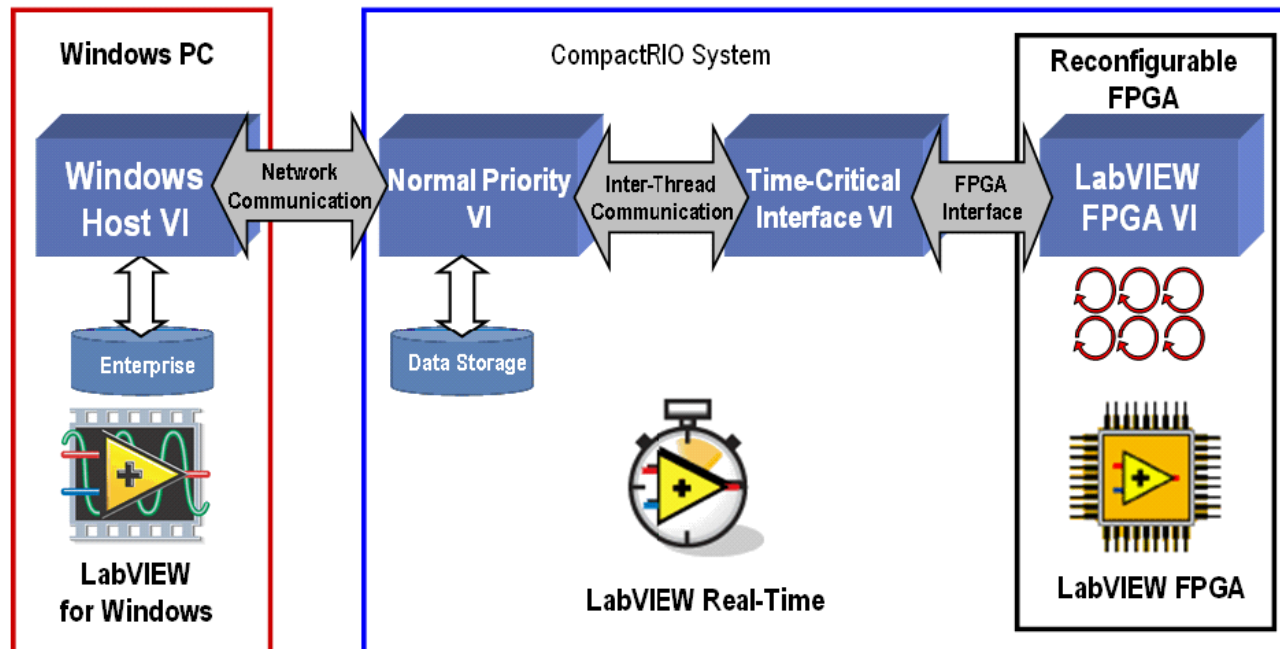


Figure 3-3: Schematic showing the architecture of how FPGA, cRIO, and Windows Systems work together [40].

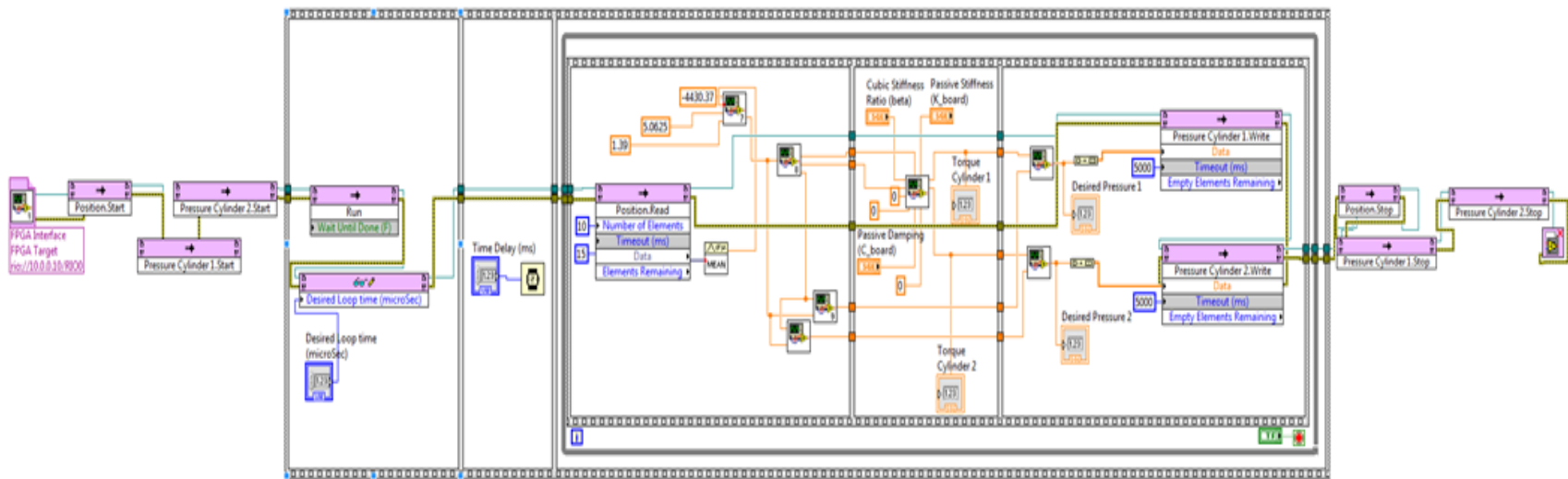


Figure 3-4: Main Labview program that uses the stiffness coefficients to calculate and control the desired pressure in each cylinder.

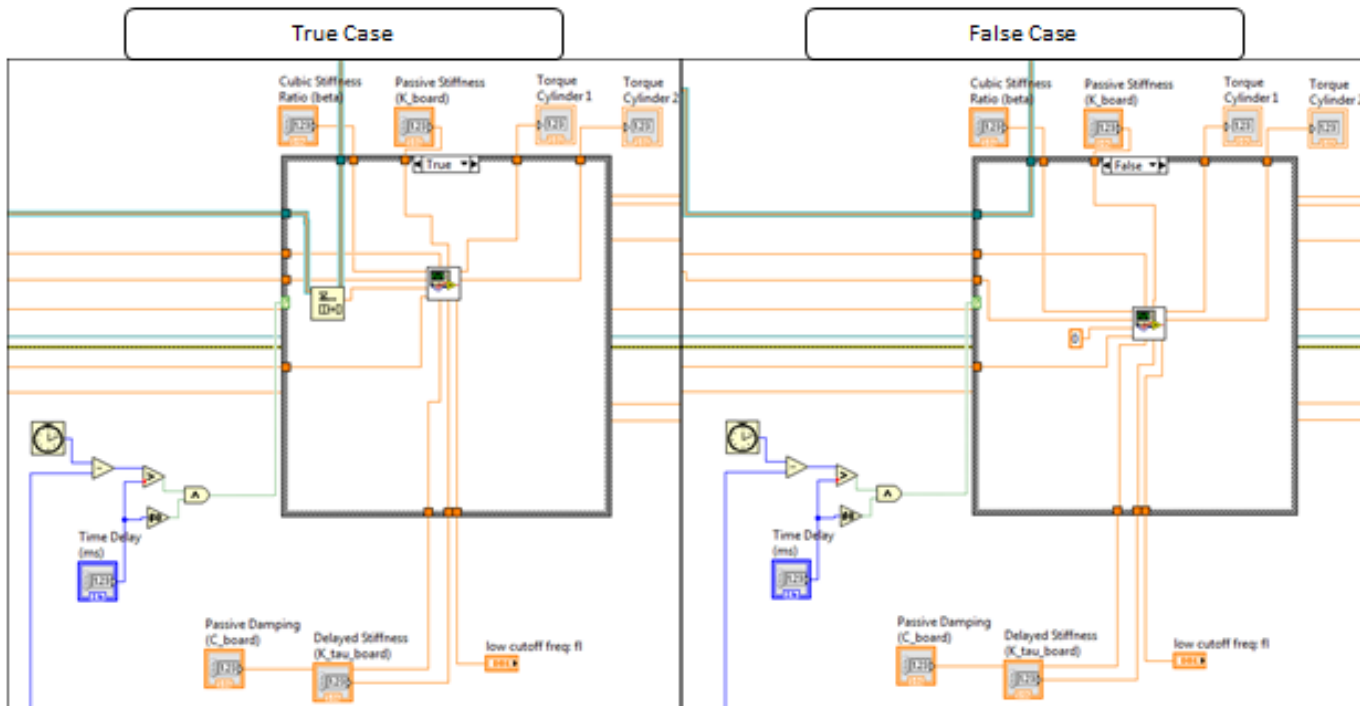


Figure 3-5: Case loop used in conjunction with memory items to incorporate the haptic feedback time delay.

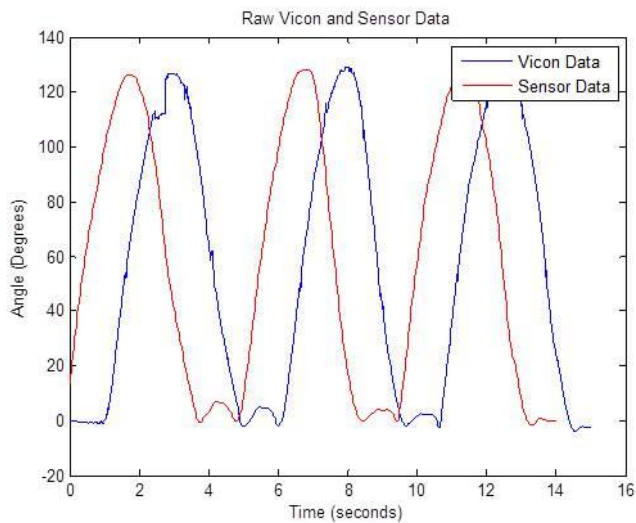


Figure 3-6: Raw data from the Vicon© and 3-Space Wireless Sensors during the three flexion-extension movement showing the change in angle between the upper and lower arm.

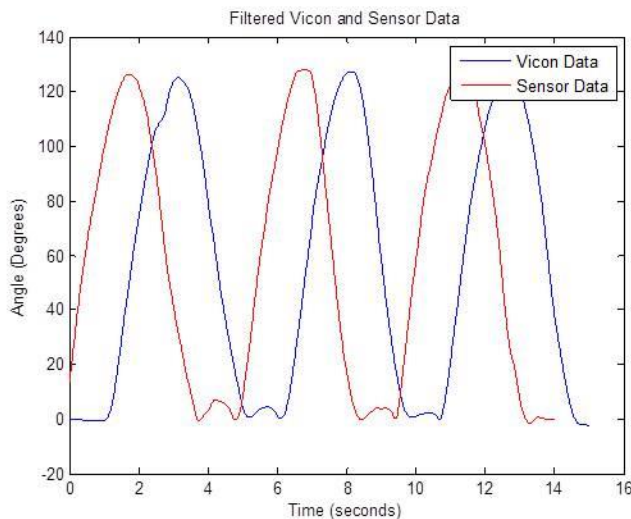


Figure 3-7: Filtered and resampled Vicon© data and Wireless Sensor data shown across time during the test.

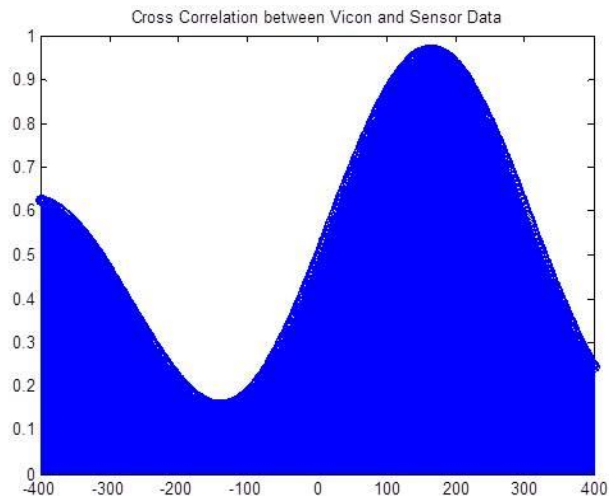


Figure 3-8: Cross correlation of the Vicon© data with the wireless sensor data.

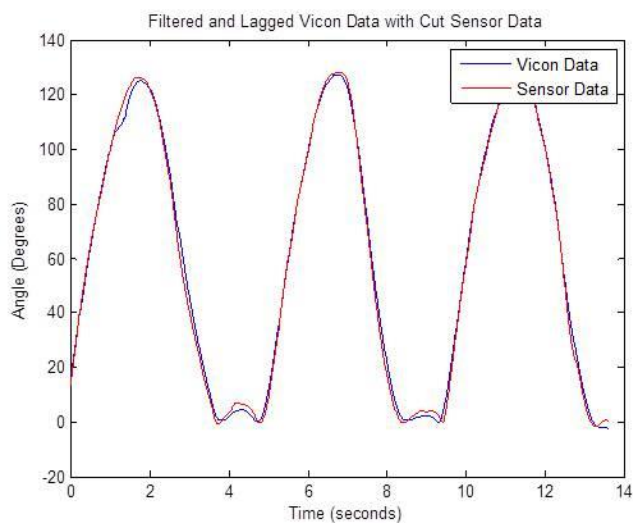


Figure 3-9: Comparison of Vicon© data and wireless sensor data once the calculated lag is applied to the Vicon© data.

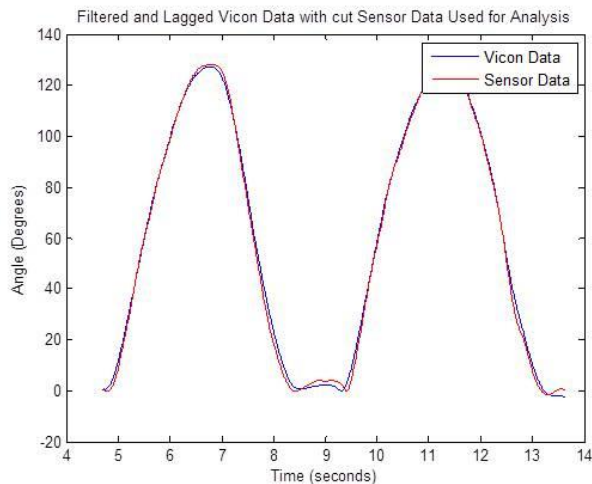


Figure 3-10: Flexion-extension data from the Vicon© and wireless sensors that was chosen to be used for validation of the wireless sensors.

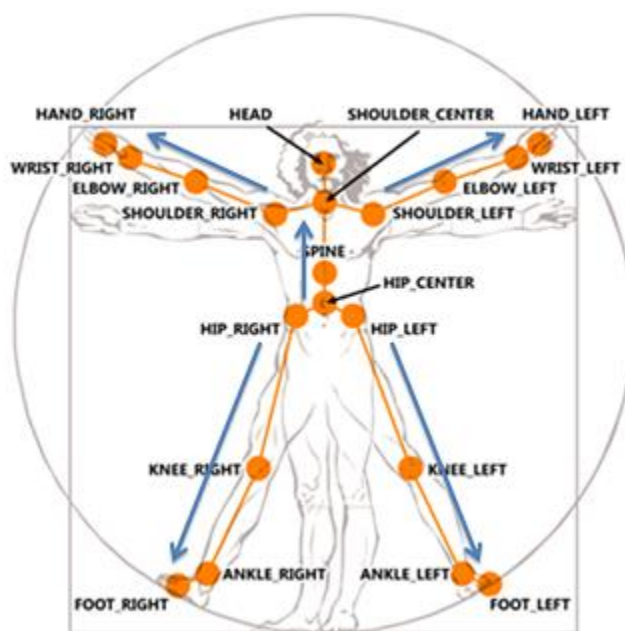


Figure 3-11: Human diagram showing specific joints that are tracked with the Skeletal Tracking program by Kinect™ [41].

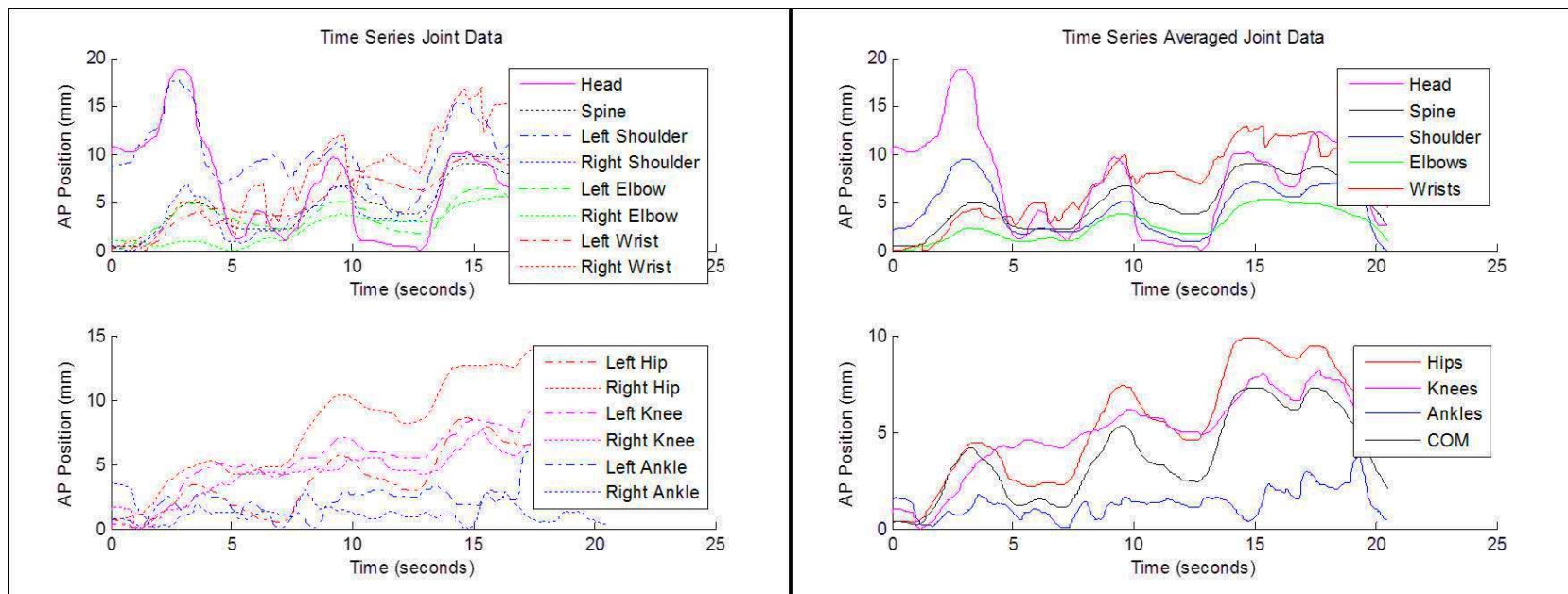


Figure 3-12: Kinect AP position data of each skeletal joint during quiet standing. Both left and right joint positions are captured and shown (left); left and right joint positions were averaged to get one value to represent each joint (right).

CHAPTER 4. MEASURING HUMAN RESPONSES

This chapter discusses the initial proof-of-concept tests that were performed with human subjects on the balance board. A preliminary analysis of the data trends are also discussed

4.1 Human Experiments

As the participants enter the lab, they were shown the balance board system, the Kinect™, and the Wireless Sensors. The instructions are read to the participant, and any questions are answered. After the participant has been informed of the expectations, and they have had all of their questions answered, informed consent is provided. At this point, we weigh the person and measure their height, and then this information is entered into the Labview™ program. This information was used to determine the stiffness and damping coefficients during the testing, which are normalized with respect to each person's weight and height. The wireless sensors were then put in place. These sensors were attached to the participant with Velcro straps at the head, the chest, the pelvis, the right thigh, and the right calf. The final sensor was placed on the balance board via Velcro; this placement gives us a simplified way to align the Labview™ data with the wireless sensor data, since both systems will be recording angle of the board.

Once the person is fitted with the wireless sensors, we check the functionality of each sensor. This is to ensure that all of the sensors are working properly, and that they have enough battery life to last through the entire test. The Kinect™ is set up behind the balance board, and it is examined to make sure that the balance board is properly in place in the video capture window. At this point, we are ready to begin the testing. There are three different tests, the first is the discrete varying torsional stiffness, the second is the continuous variable torsional stiffness, and the third is the variable haptic feedback time delay.

For both of the varying torsional stiffness tests, the balance board is initially placed at a maximum torsional stiffness value, and a maximum damping coefficient value, which makes the board feel like a rigid platform. These values are both decreased until they are zero, and then, to test for hysteresis, we increase both of the coefficients until they are again at their maximum values. This test was completed in two different manners: the first decreases and then increases the varying quantities with discrete step sizes, the second implements a linear ramp down, and then a linear ramp back up. The step size for the first type of test was determined to be ten percent of the maximum values. These two methods are described in more detail below.

For both of the variable torsional stiffness tests, the maximum values were the same. The maximum torsional stiffness value was determined to be 5 times the critical stiffness value, K^{cr} , which was defined in Chapter Three as mgh ; m is the participant's mass, g is gravity, and h is the height of the center of mass

of the person. The damping coefficient is set to 20% of K^{cr} , and the cubic stiffness coefficient is set to 5% of K^{cr} . These values were decided upon after analysis of previous modeling and simulations, as well as extensive pilot testing with people of various weights and heights.

With the board parameters set at the maximum, the participant is told to use the handrails to step up onto the board. Once on the board, they are told to align their ankles with the central line drawn on the board, which indicates the pivot point of the board. The feet location is marked with tape so that they have constant foot placement throughout all of the testing. The participant is instructed to look at a sticker placed directly in front of them on the wall, and to keep the board perfectly horizontal throughout the test. They are reminded that the stiffness of the board will decrease and then increase over time. The person is instructed to only use the hand rails if they feel like they are going to fall.

For the stiffness test with discrete decrements/increments, there are ten discrete decrements in board stiffness, and then ten discrete increments, each lasting ten seconds. The total stiffness test on a subject thus takes 210 seconds, or 3 minutes and 30 seconds. After test completion, the participant is told to step off of the board, and is allowed a rest period of three minutes. We repeat this process three more times, leading to the test being repeated a total of four times.

The continuous stiffness ramp test is very similar to the discrete step size test, except that the torsional stiffness and damping coefficient values decrease very smoothly from the maximum to zero, and then increase smoothly back up to the maximum values. The entire process takes about three and a half minutes,

and it is accomplished by changing the desired values by 0.02% every loop, which takes 6 milliseconds. This test was repeated for four trials, with three minute breaks in between each trial.

During both variable torsional stiffness tests, a person should lose upright postural stability as the stiffness values decrease, allowing the board to lean. Once stiffness values are increased, a person should regain the ability to maintain upright posture, and at this point the board should be kept in a horizontal position. The two tests are being done to see if a person experiences a different instability point based on whether the change in stability is discrete or continuous.

The next test is the variable haptic feedback time delay in the balance board. For this test, the values of the coefficients needed are different than they were for the variable torsional stiffness test; specifically, the torsional stiffness is set to 75% of K^{cr} , the delayed stiffness is set to 1.7 times K^{cr} , the cubic stiffness is set to 5% of K^{cr} , and the damping coefficient is set to 5% of K^{cr} . These values were determined after completing pilot testing.

During this test, the parameters are set as discussed above, and then the participants step onto the balance board. Once they are comfortable standing, the test begins. The time delay of the board is initially set to zero, and then every ten seconds it is increased by 50 milliseconds. This continues until the time delay reaches 300 milliseconds. At this point, the time delay is decreased by 50 milliseconds every 10 seconds, until it arrives back at zero.

This test takes 130 seconds, or two minutes and 10 seconds. The test is repeated four times, with two minute breaks in between each trial. During this test, we expect to see people lose stability at some critical time delay value. Their loss of stability should be via a limit cycle oscillation, and then as we decrease time delay, they should reenter their stability region.

We received IRB approval for this human research; reference number: 1305013578. The entire procedure, including instructions given to participants and exact timing of each step can be found in the Appendix.

4.2 Observation of Two Mechanisms of Instability

One of the main goals in the initial testing was to observe the outcomes of the two distinct mechanisms of instability: leaning forward or backward and limit cycle oscillatory behavior. Both of these behaviors were seen during testing, proving that the board is capable of eliciting both mechanisms of instability.

4.2.1 Forward/Backward Leaning

During the variable discrete step torsional stiffness testing, we observed bifurcations to forward and backward leaning in all of the participants. The participants are shown losing upright stability as torsional stiffness approaches zero, and leaning either forward or backward (Figure 4-1). Subjects do not remain in leaning positions but rather try to recover their balance intermittently. As the stiffness increases towards its maximum, the zero degree position again becomes a stable point, and the participants are able to maintain the board in this horizontal position.

This is a promising result because it confirms the prediction from the model. Seeing this forward/backward leaning is crucial because it confirms that the board is capable of utilizing this first mechanism of instability in human participants.

4.2.2 Limit Cycle Oscillations

During the variable time delay test, we witnessed the limit cycle oscillatory behavior that we were expecting (Figure 4-2). As the time delay increases, we start to see intermittent limit cycles, and when the time delay is again set to zero, the participant tends to regain stability.

Because the stiffness and damping values were set below the upright stability point for each participant, at the beginning of the test we tended to see some forward/backward leaning due to the first mechanism of instability. As the test went on, and the time delay value was increased, limit cycle oscillatory behavior tended to occur.

4.3 Transient Human Response

By closely observing the response from the discrete torsional stiffness test (Figure 4-1), one can see transient portions of the human response as the stiffness and damping values are changed in a discrete manner. Because the step sizes are relatively large, at 10% of the maximum values, and they are discrete, there is a distinct transient response from the participant as the values are changed. One way to deal with this issue is to perform a linear ramping torsional stiffness test rather than a discrete step stiffness test. The participants' response to a linearly varying torsional stiffness test is shown (Figure 4-3).

This test is interesting because without the discrete stepping of the torsional stiffness values, there is no transient portion of the response. Although the range of the torsional stiffness values was the same for both the discrete step test and the linear ramping test, we see different responses from the participants.

4.3.1 Alternate Testing Procedure

After examining the results from the discrete step torsional stiffness test, shown in Figure 4-1, we noticed a transient portion of the participant response each time the stiffness value was changed. Because each stiffness value was only maintained for ten seconds, the participant did not have much time to move into a true steady state behavior. One interesting behavior to look at would be the residence time that we maintain each stiffness value. If we increased this residence time, it would give the participants an opportunity to reach a more steady state behavior.

Another interesting experiment considered after the initial results were analyzed was to decrease the amplitude of the torsional stiffness value change. Different trials of the test would continue to decrease the change in stiffness at each step value. This would be interesting because it would give insight about what amplitude of torsional stiffness value is needed to achieve a response similar to that of the linear ramping stiffness test (Figure 4-3). It would be possible to determine at what step size we see a loss of transient behavior.

4.4 Degrees of Freedom

Viewing the person as a single segment inverted pendulum leads to a single degree of freedom system. If the person's only pivot point is at the ankle,

then this assumption of a single degree of freedom system is valid; however, if the person flexes/extends at multiple joints in an effort to regain upright stability, then the model is no longer valid. During the human experiments, 3-Space Wireless Sensors by YEI Technology were placed on each person's head, chest, waist, thigh, and shin. An additional sensor was placed on the balance board. The data gathered by the wireless sensors during the linear ramping stiffness test is shown (Figure 4-4).

The sensor data can be critically examined to determine if specific body segments are moving in the same direction as other body segments. In the top portion of the graph (Figure 4-4), we generally see that as the board moves, there is not much movement from other body segments; this suggests an ankle strategy that aligns with the model. However, for some board movements, there is also movement in the shin, but not in any other body segments, which suggests a knee-bending strategy. At the point of the highest board angle, all segments of the body move in a similar manner. This tells us that the participant lost upright stability, and leaned the whole body forward. Movements like this will need to be quantitatively analyzed to determine if there is a significant difference compared to the behavior the model predicts.

The center panel of the graph (Figure 4-4) shows participant two's kinematics. There are a few examples of only the board angle changing, suggesting the ankle strategy, but in this participant it is much more common for all body segments to be moving simultaneously. This suggests that the

participant did not consistently maintain a vertical upright position. Further conclusions cannot be made just by observation of this data.

Lastly, the bottom panel of the graph (Figure 4-4) shows the kinematic behavior of participant three. The primary strategy observed in this case seems to be bending of the knee: the shin and board angles tend to be similar, but the thigh angle opposes the board/shin angle.

This thorough initial examination of the sensor data shows a wide range of strategies for balancing on the board. This variation suggests that a simple model with the only pivot at the ankle joint may not be valid for a person standing on the balance board.

For quantitative results, joint angles were calculated from the sensor data (Figure 4-5). The top panel of this graph shows the behavior of the first participant. Here the primary movement is via the ankle, indicating an ankle strategy for maintaining upright posture. The center panel of the graph shows large ankle, knee, hip, and waist angles. This participant did not seem to have a primary strategy for maintaining the upright position. Because of this, it is fair to assume that for this specific participant, the single segment inverted pendulum model would not fully represent the dynamics of movement. Lastly, the bottom panel of the graph shows substantial ankle movement, in addition to hip and waist movement. It can be assumed that participant three was using a combination of an ankle strategy and a hip strategy to remain upright.

4.5 Conclusions

Proof-of-concept tests with human subjects clearly show that both mechanisms of instability can be observed. The behaviors showed similarities to, the model's predictions, but unexpected movements were also observed, which suggests that a person may change his/her balance strategy if their initial strategy is not working properly. For example, the model predicts that if a person becomes unstable via the forward/backward leaning mechanism, they would stay offset from zero until the stiffness is returned to some critical value. However, we see that the person does not stay in one angular position, but instead tries to reinstate a horizontal board position, leading to leaning in the other angular direction. This suggests that multiple strategies are involved in maintaining upright posture, especially as the person loses stability. Overall, the analysis of the results led to ideas for new tests to run to learn even more about the participants' behavior on the balance board.

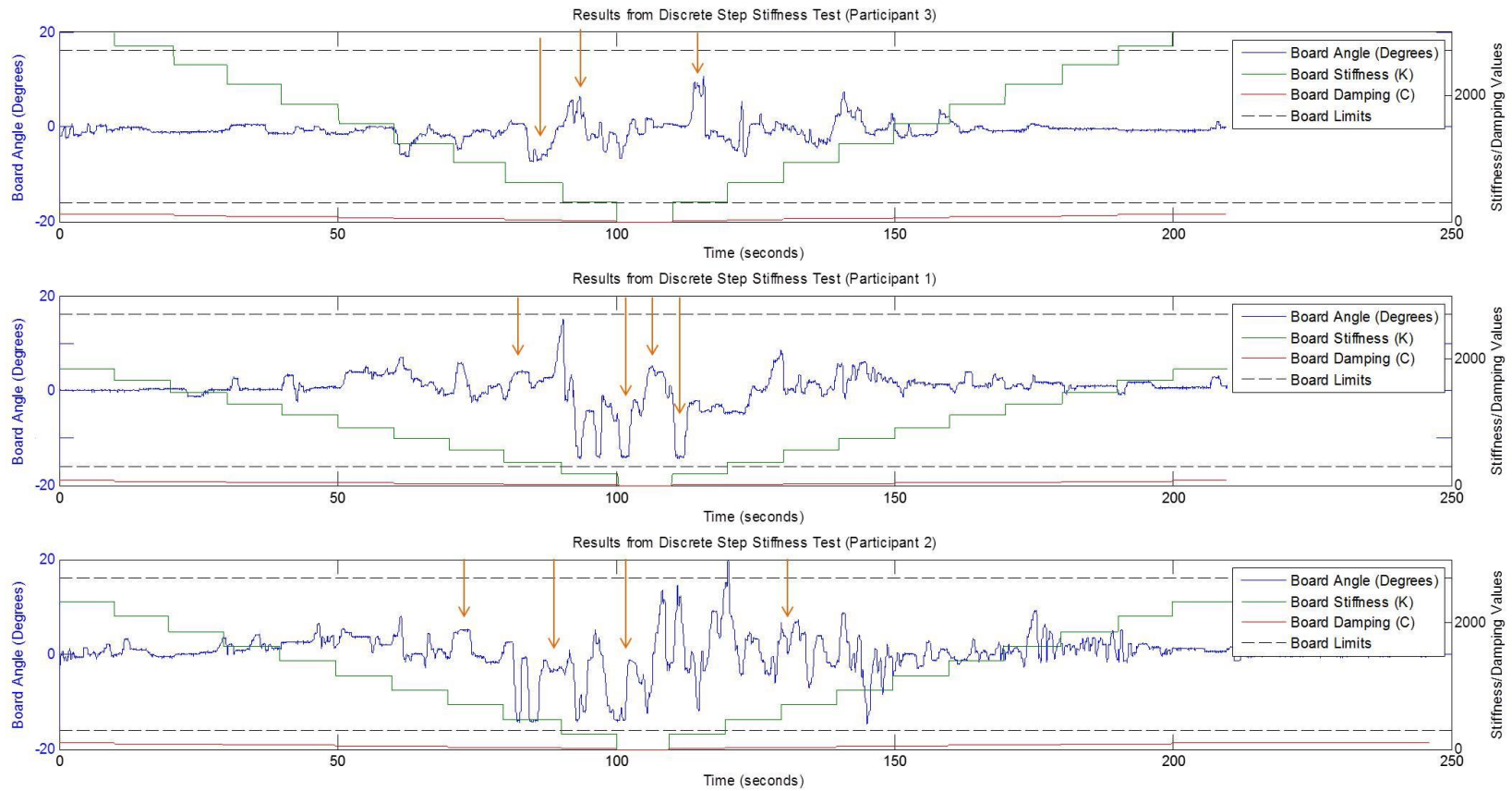


Figure 4-1: Results from all three participants performing the discrete step stiffness test. One can observe an initial leaning response in all of the participants as stiffness and damping approach minimum values, and high levels of movement as they try to recover their balance. Periods of leaning are highlighted with orange arrows. There is a return to upright stability as the stiffness and damping values approach their maximums.

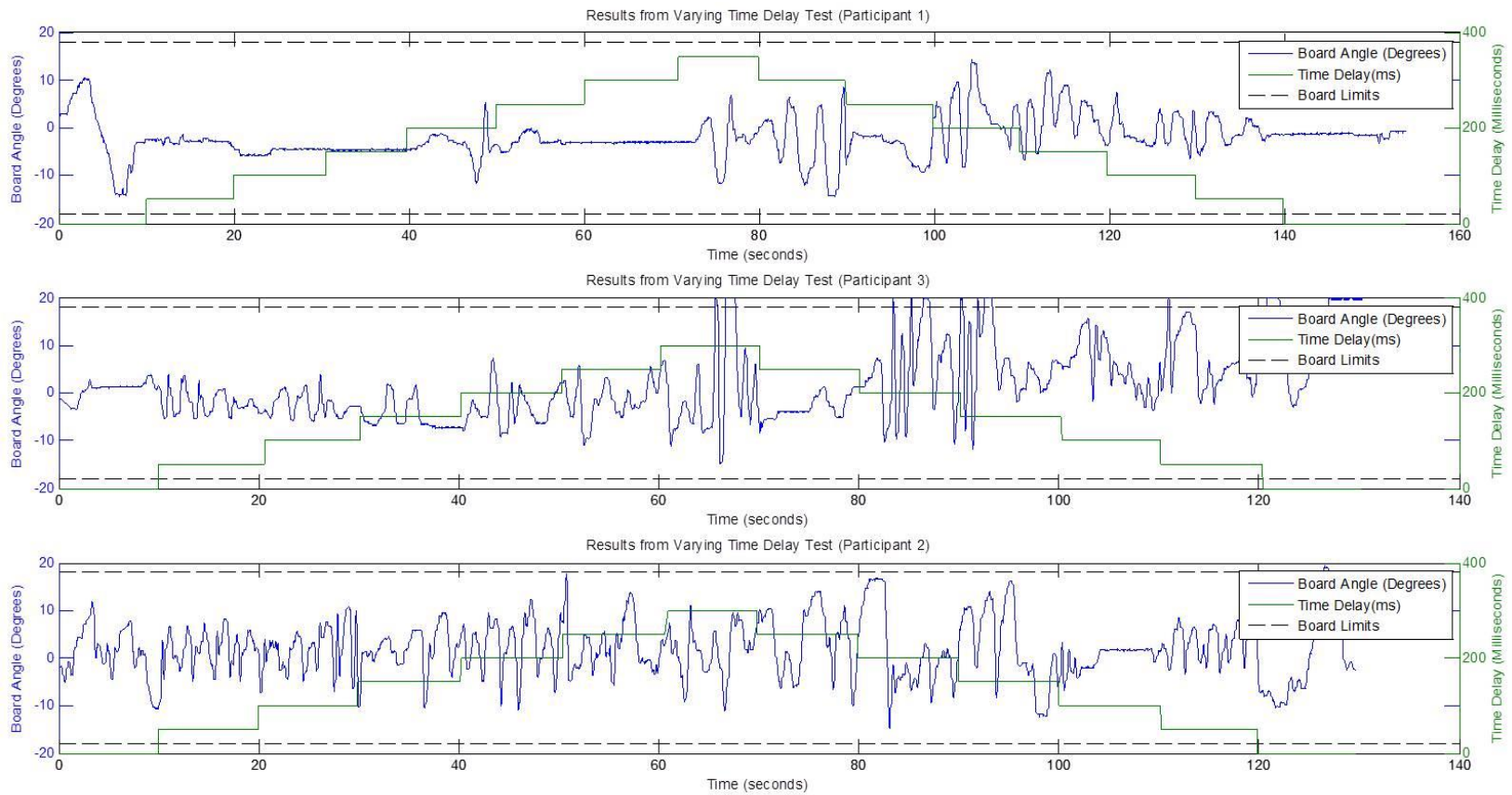


Figure 4-2: Results from all three participants performing the variable time delay test. It can be seen that limit cycles tend to occur as the time delay approaches its maximum value, as highlighted by the orange arrows. Most participants are able to avoid the limit cycle behavior at low time delay values.

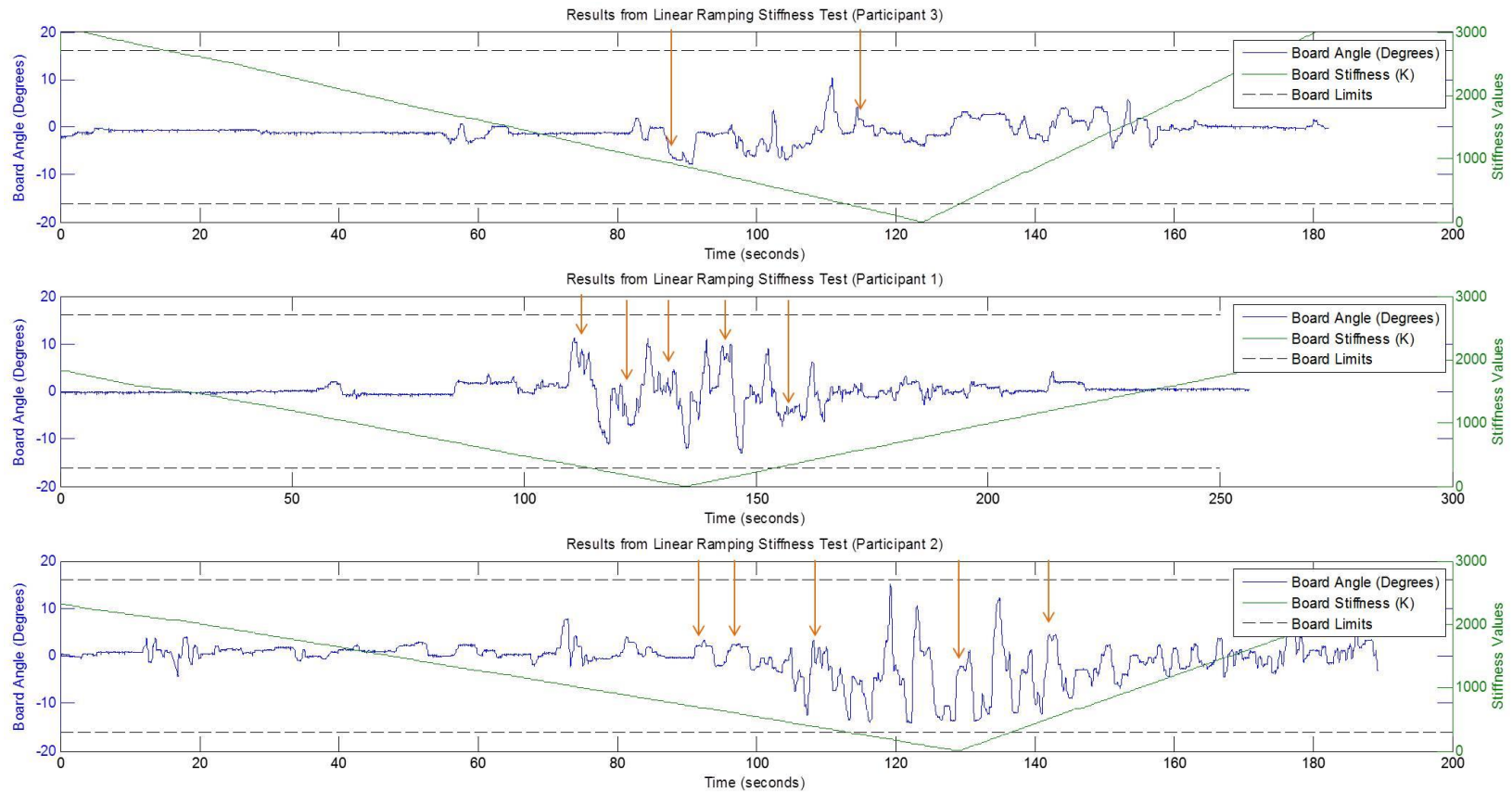


Figure 4-3: Results from all three participants performing the linear ramping torsional stiffness test. We see the behavior that we expect with loss of upright stability leading to forward/backward leaning, indicated with orange arrows, when stiffness approaches a minimum.

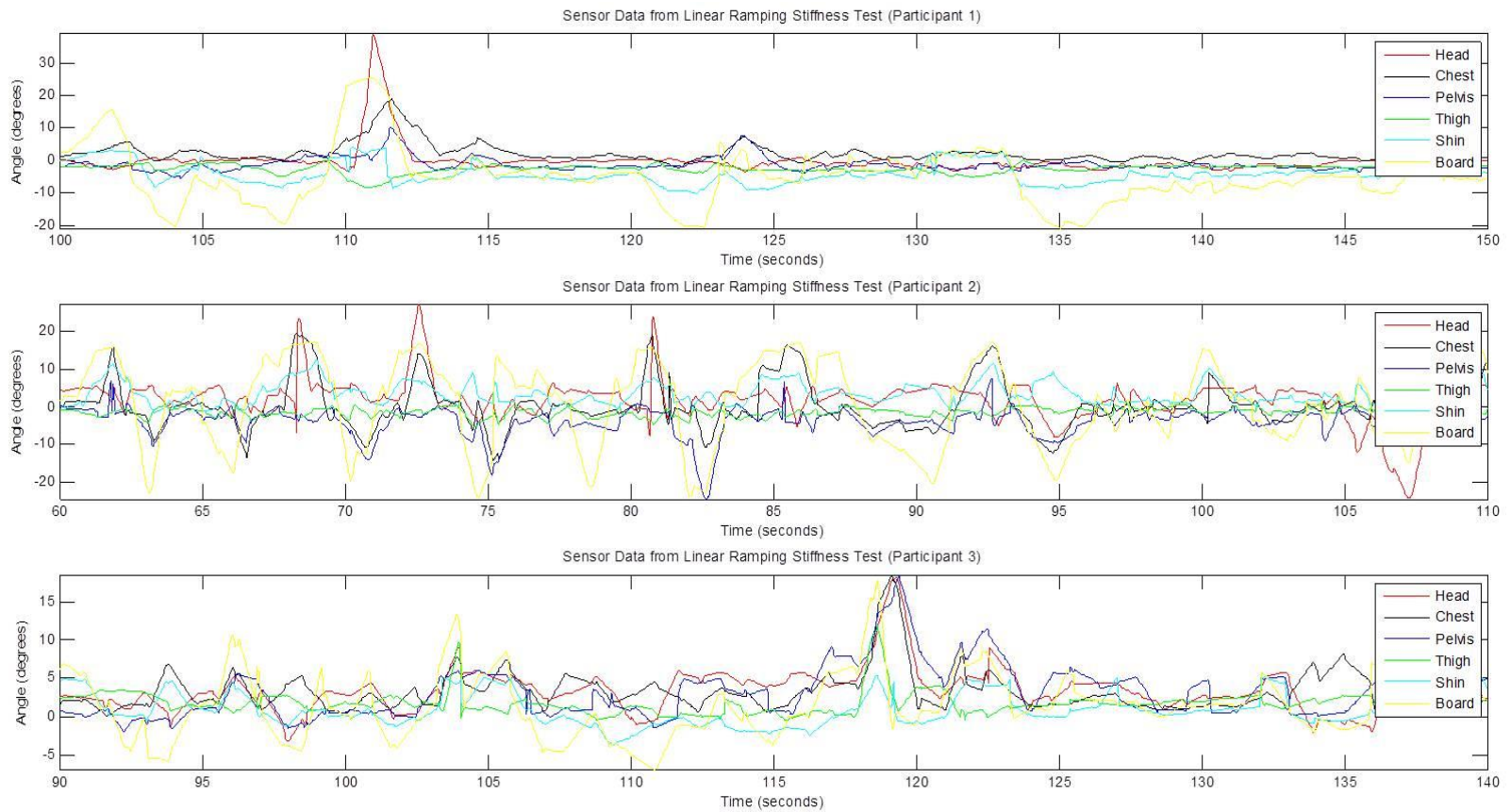


Figure 4-4: Sensor data from all three participants during the linear ramping stiffness test. Sensors were placed on the head, chest, pelvis, thigh, shin, and balance board.

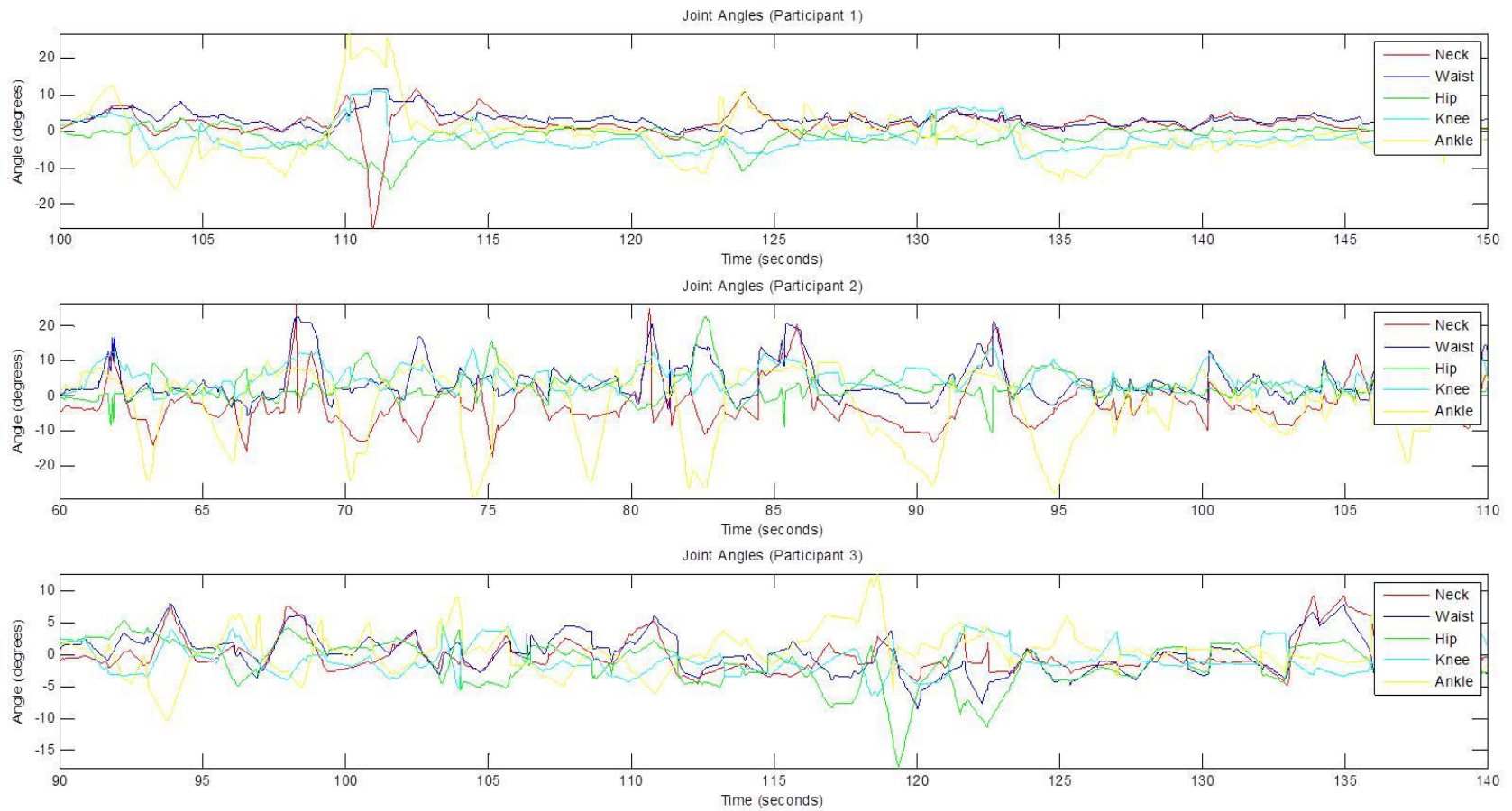


Figure 4-5: Joint angles calculated with the sensor data from all three participants during the linear ramping stiffness test. This data shows that the three participants each use different balancing strategies.

CHAPTER 5. CONCLUSIONS AND FUTURE WORK

This chapter reviews the main accomplishments of this research. In addition to this review, ideas of things to be studied in the future will also be discussed.

5.1 Balance Devices

As was previously discussed, the ability to maintain upright posture can decline for a variety of reasons, including aging and several types of diseases, especially neuromuscular disorders [4], [6]. Fortunately, research has found that balance training can be very effective in improving static postural sway and dynamic balance [9]. The devices typically used for balance training are passive wobble boards, the Biodex System SD®, and the Neurocom SMART Balance Master®. Although these devices do help to improve balance, they only utilize one mechanism of instability, seen via forward or backward leaning. It has been found that there are two distinct mechanisms of instability which have different behavior outcomes: forward/backward leaning, and limit cycle oscillations [24]. In order to detect all types of balance disorders, and in an effort to improve more than one type of instability, we have built a balance board that utilizes both mechanisms of instability.

5.1.1 Review of the Balance Board System

The novel balance board system, which moves 15 degrees with one degree of freedom, is able to induce both types of instability by having two variable parameters. The first is common in balance devices: torsional stiffness. As torsional stiffness is decreased, it becomes more difficult to maintain upright stability, and we see that a person will lean either forward or backward. The second variable parameter is haptic time delay. As this haptic feedback time delay of the board is increased, we see limit cycles oscillations arise.

This ability to utilize both mechanisms of instability is useful because it gives us more information about the type of balance issues the participant is experiencing, and this information may increase the likelihood of being able to help improve the person's balance.

5.1.2 Tactile Response Platform

There are balance devices in addition to balance boards that can help various populations improve their balance. If a loss of balance is due to peripheral neuropathy or cutaneous sensory deficits, which is often true in patients with diabetes, the patients have deficiencies in both their sensory and motor abilities [42]. Although the cause of the decline in balance may be different than in other cases, it has been shown that specific training can improve a variety of issues in diabetic patients, including balance, muscle strength, and joint mobility [43]. One type of training that has been explored is providing the patient with input noise to help enhance his/her sensorimotor function. The idea behind this is a phenomenon called stochastic resonance: it shows that added noise is

able to enhance the transmission of weak signals in sensory systems. Vibrating insoles are an implementation of this idea, and have been shown to significantly reduced postural sway [44].

This work is extremely exciting, and it is an example of a way of exploring different mechanisms of instability, along with ways to help improve this deficiency. Our group is interested in creating a device that can be used to diagnose and treat individuals who may experience balance insufficiencies due to peripheral neuropathy, primarily due to diabetes. Perhaps we could combine the current balance board with a device of this type in order to diagnose and train multiple distinct mechanisms of instability.

5.1.3 Robotic Balance Platform

The novel balance board system is currently able to record data, but results concerning the participant's balancing abilities need to be determined after post-processing of the data. It would be advantageous to have a system that could analyze data in real time, and then use this analysis to create individualized training procedures. This idea is contained in the field of machine learning, which focuses on three primary areas: task-oriented studies, cognitive simulation, and theoretical analysis [45]. The machine-learning controller would have to determine where a person's limit of stability is for each mechanism of stability, and then create a training plan that utilizes this knowledge. This would be an example of a task-oriented study. To implement this type of software into the system, first it is necessary to perform a large number of human studies and analyze the data to determine if there are common trends between participants. It

is also necessary to confirm if training on a balance board with variable torsional stiffness and time delay is able to help improve stability with regards to both instability mechanisms. This is a desirable goal because it would give people with poor balancing abilities a novel tool that would help them improve their balance more efficiently than other systems that are currently on the market.

5.2 Human Testing

We initially completed three rounds of pilot testing which helped us to determine the values of the stiffness and damping coefficients. These tests also helped us to create the procedures for the three tests: discrete step stiffness test, linear ramping stiffness test, and variable time delay test. Once we had finished pilot testing, and felt that the procedures were sufficient for all three tests, we proceeded with the initial human testing. Three participants were recruited for this initial round of testing, and every participant performed four runs of each of the three tests. This provided sufficient data for initial analysis. The full procedure for the human testing can be seen in the Appendix.

5.2.1 Conclusions from Initial Testing

We successfully completed the three tests with all three participants, and we were able to gather data for each of the tests. Forward/backward leaning was observed during the variable torsional stiffness testing, as the stiffness value was decreased to a critical value. This is shown in Figure 5-1.

This discrete step stiffness test ran as expected, although one general improvement that we should make is to muffle the sound of the valves during the test. Because we have discrete steps, a large amount of air is being released or

added every ten seconds. A loud noise occurs whenever large amounts of air are moved through the valves; this noise lets the participant know that a change is being made in the stiffness of the board. We do not want the participants to know when the values are being changed, so it would be ideal if we could fully muffle the noise before we complete any future testing.

Another interesting observation made from the discrete step stiffness test was that there is some transient response to the stiffness being changed. This can be verified by comparing the discrete step stiffness data to data from the linear ramping stiffness test (Figure 5-2).

Without discrete steps to change the stiffness values, the results are more similar to what is expected based on the model's predictions (Figure 5-2). There are clear regions where the person on the board is in a leaning instability, and cannot bring themselves back to the upright position at zero degrees. These plateaus at various angles disappear when stiffness is again high enough for the person to maintain upright stability with the board in a horizontal position.

After observing the linear ramping stiffness test, we identified some things changes to implement before we test again. The primary issue that we noted was that the stiffness took longer to ramp down than it did to ramp back up. We were changing the value by a constant percentage in each loop; this discrepancy tells us that the loop times are not consistent. We had a loop timer control set at two milliseconds, so this tells us that the loop is taking longer than two milliseconds. Before the next test, we need to measure exactly how long the loop takes to execute, and then set the loop timer control to be greater than this value. If the

loop is taking too long to execute, we will have to improve the efficiency of the code so that it runs more quickly.

The second mechanism of instability, identified via limit cycle oscillations, was also observed. This was induced in participants during the varying time delay test. Because the stiffness and damping values were set below the upright stability point for each participant, at the beginning of the test we tended to see some forward/backward leaning due to the first mechanism of instability. As the feedback time delay increased, we started to observe intermittent limit cycles (Figure 5-3).

After performing the variable time delay tests, we discovered several improvements that could be made to the procedure. As participants went into intermittent limit cycles, they seemed uncomfortable; this was due to the amplitude of the limit cycles being larger than desired. To fix this problem, we should increase the cubic stiffness coefficient and the damping coefficient. We will need to do some experimental testing to determine what the new values will be for these coefficients. We should reduce the overall angular range of the board, so that a person cannot tilt in either direction more than ten degrees.

Based on the data shown in Figure 5-3, we are also interested in performing a similar test, but staying at each time delay value for a longer period of time. It is suspected that when the time delay value is changed, the person experiences some transient response. The steady state response that should follow this transience is more interesting to us, but it not visible within the ten

seconds at each time delay value. Lengthening the amount of time at each time delay value will be an upcoming test that we will complete.

5.2.2 Alternate Populations

The initial human testing has only covered healthy, college-aged participants. We would like to increase the breadth of our knowledge by testing various other populations on the board. There is a direct link between aging and a decline in balancing abilities, so testing older adults would be the next group that we would be interested in. This would give us greater knowledge about people with varying decreasing levels of stability. To study the higher end of balancing abilities, it would be interesting to study athletes. One potential interest would be to compare athletes to age-matched participants, and then also compare various sports to determine if some sports improve a person's balancing ability more than others.

Once this range of testing is complete, and any necessary modifications to the procedure and/or balance board have been made, we are interested in testing people with neuromuscular disorders. Studies have shown that intermittent limit cycles can be seen in people with neuromuscular disorders, specifically multiple sclerosis (MS) and concussions, even while standing on a rigid surface [24]. We hope that because the balance board has controllable haptic time delay, we would be able to detect limit cycles in patients with even a slightly elevated neuromuscular time delay. To test this, we would need a participant pool of people with neuromuscular disorders. Acute disorders, such as concussions, are especially interesting because then we can compare the

results after they have recovered from the concussion—it would be expected that the limit cycle behavior disappears after a full recovery.

5.2.3 Additional Goals of Subject Testing

One of the primary goals with the balance board system is to use it as a training device. To do this, we first need to determine if a person improves more rapidly on our board than on a passive balance board, or on a board that is already on the market. We will need to study people on our balance board over several weeks to study if their balance improves over time as they are using the board.

Another potential ability of our balance board would be to create a quantitative balance score for the user. This would be normalized so that it could be compared between population groups who would be expected to have similar balancing abilities. If this were possible, we may be able to identify if a person had a balance score lower than expected; this would be a sign that the person should begin balance training, and perhaps see a medical professional to determine potential reasons for their reduced balancing ability.

5.3 Overall Conclusions

This thesis has described the process of designing and creating a novel balance board with variable torsional stiffness and time delay. This balance board is a novel product that has the potential to improve the ability to diagnose and improve balance instabilities. The balance board has been proven to be functional by performing an initial round of human testing. This testing has shown that our balance board system is capable of detecting two distinct mechanisms of

instability by observing forward/backward leaning and limit cycle oscillations. Now that this initial testing has proved basic functionality of the balance board, additional testing can be started in order to explore alternate areas of balance research.

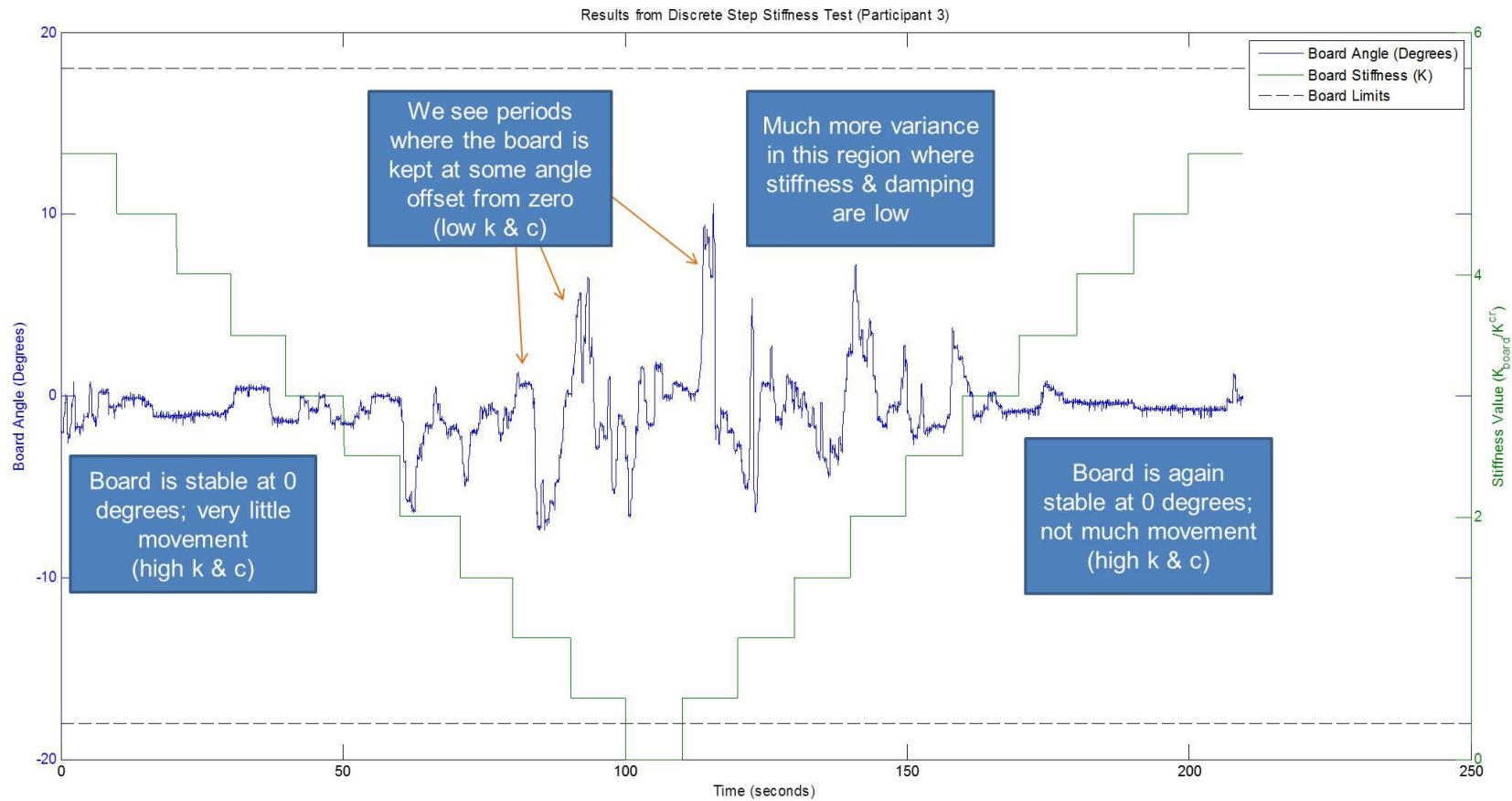


Figure 5-1: Discrete step stiffness test results showing the controlled change in stiffness and damping coefficients, as well as the resulting change in board angle over the time length of the test.

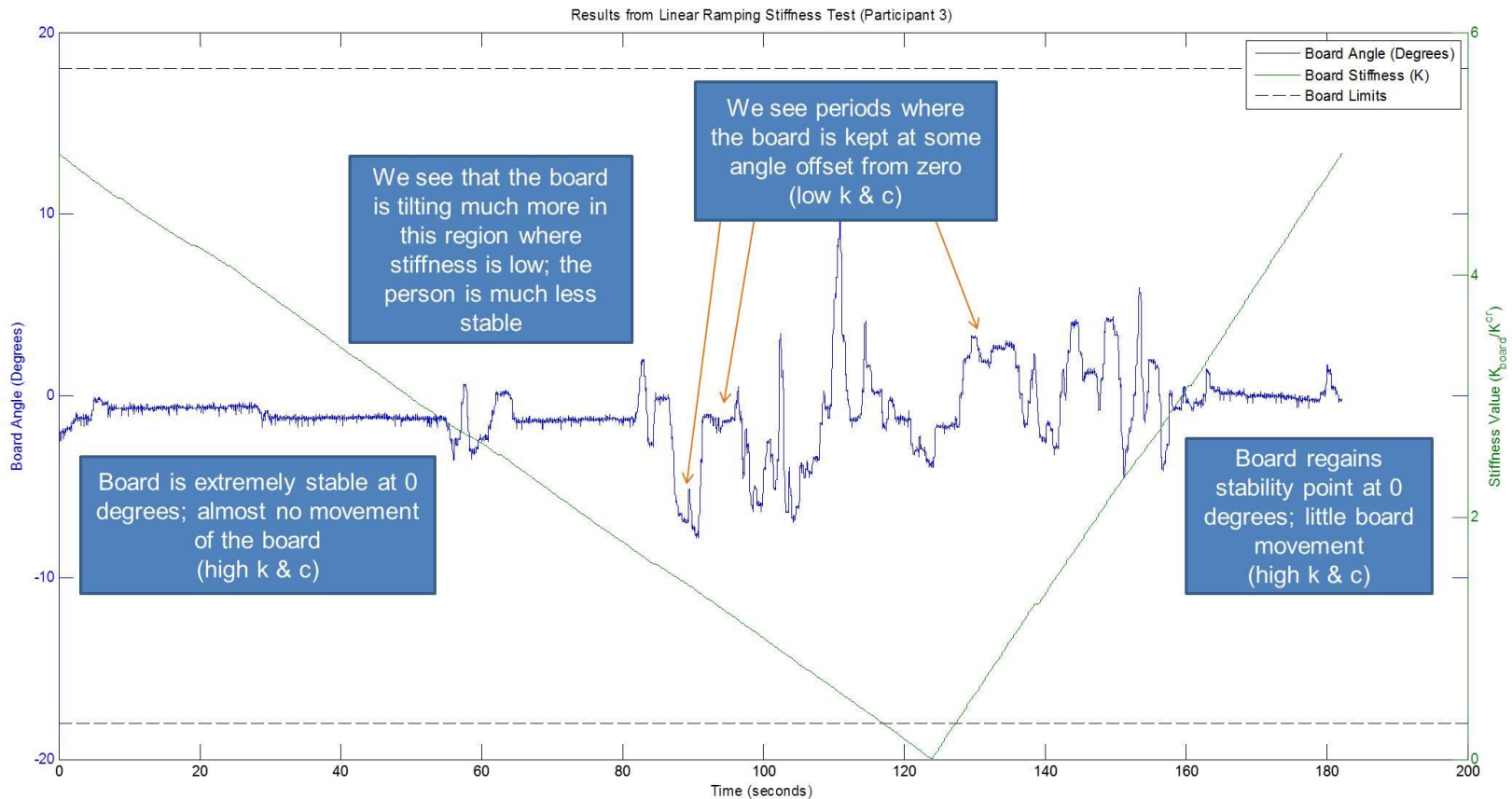


Figure 5-2: Linear ramping stiffness test results, showing how the participant moved the board as the stiffness coefficient was changed.

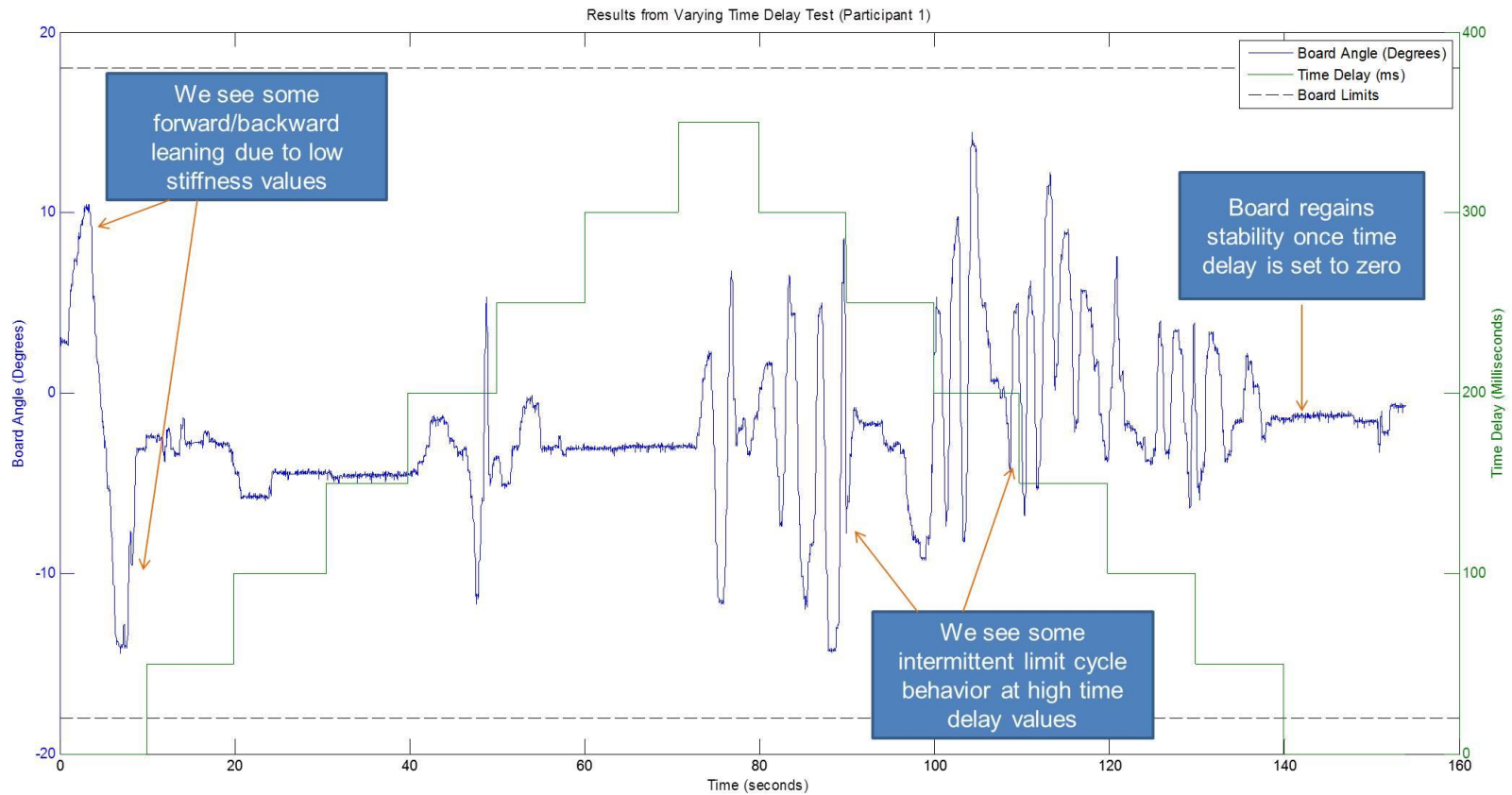


Figure 5-3: Variable time delay test results, showing limit cycle oscillations as time delay is increased past some critical value, and a return to upright stability as time delay is again set to zero.

LIST OF REFERENCES

LIST OF REFERENCES

- [1] J. R. Chagdes, S. Rietdyk, M. H. Jeffrey, N. Z. Howard, and A. Raman, "Dynamic stability of a human standing on a balance board," *J. Biomech.*, 2013.
- [2] B. W. Verdaasdonk, H. F. J. M. Koopman, S. A. van Gils, and F. C. T. van der Helm, "Bifurcation and stability analysis in musculoskeletal systems: a study in human stance," *Biol. Cybern.*, vol. 91, no. 1, pp. 48–62, Jul. 2004.
- [3] F. B. Horak, "Postural orientation and equilibrium: what do we need to know about neural control of balance to prevent falls?," *Age Ageing*, vol. 35, no. suppl 2, pp. ii7–ii11, Sep. 2006.
- [4] J. O. Judge, M. B. King, R. Whipple, J. Clive, and L. I. W. Son, "Dynamic Balance in Older Persons: Effects of Reduced Visual and Proprioceptive Input," *J. Gerontol. A. Biol. Sci. Med. Sci.*, vol. 50A, no. 5, pp. M263–M270, Sep. 1995.
- [5] I. Poulain and G. Giraudet, "Age-related changes of visual contribution in posture control," *Gait Posture*, vol. 27, no. 1, pp. 1–7, Jan. 2008.
- [6] H. Stolze, S. Klebe, C. Zechlin, C. Baecker, L. Friege, and P. D. G. Deuschl, "Falls in frequent neurological diseases," *J. Neurol.*, vol. 251, no. 1, pp. 79–84, Jan. 2004.
- [7] A. J. Blake, K. Morgan, M. J. Bendall, H. Dallosso, S. B. Ebrahim, T. H. Arie, P. H. Fentem, and E. J. Bassey, "Falls by elderly people at home: prevalence and associated factors," *Age Ageing*, vol. 17, no. 6, pp. 365–372, Nov. 1988.
- [8] G. J. Azar and A. H. Lawton, "Gait and Stepping as Factors in the Frequent Falls of Elderly Women," *The Gerontologist*, vol. 4, no. 2 Part 1, pp. 83–84, Jun. 1964.
- [9] A. Zech, M. Hubscher, L. Vogt, W. Banzer, F. Hansel, and K. Pfeifer, "Balance Training for Neuromuscular Control and Performance Enhancement: A Systematic Review," *J. Athl. Train.*, vol. 45, no. 4, pp. 392–403, 2010.

- [10] R. J. Peterka, "Sensorimotor Integration in Human Postural Control," *J. Neurophysiol.*, vol. 88, no. 3, pp. 1097–1118, Sep. 2002.
- [11] L. M. Nashner, "Vestibular postural control model," *Kybernetik*, vol. 10, no. 2, pp. 106–110, Feb. 1972.
- [12] A. Shumway-Cook and F. B. Horak, "Assessing the Influence of Sensory Interaction on Balance Suggestion from the Field," *Phys. Ther.*, vol. 66, no. 10, pp. 1548–1550, Oct. 1986.
- [13] Elizabeth O. Johnson and Panayotis N. Soucacos, "Proprioception," *International Encyclopedia of Rehabilitation*. 2010.
- [14] S. Wapner and H. A. Witkin, "The Rôle of Visual Factors in the Maintenance of Body-Balance," *Am. J. Psychol.*, vol. 63, no. 3, pp. 385–408, Jul. 1950.
- [15] G. Wu and J.-H. Chiang, "The significance of somatosensory stimulations to the human foot in the control of postural reflexes," *Exp. Brain Res.*, vol. 114, no. 1, pp. 163–169, Mar. 1997.
- [16] P. A. Fransson, S. Gomez, M. Patel, and L. Johansson, "Changes in multi-segmented body movements and EMG activity while standing on firm and foam support surfaces," *Eur. J. Appl. Physiol.*, vol. 101, no. 1, pp. 81–89, Sep. 2007.
- [17] Aaltonen S, Karjalainen H, Heinonen A, Parkkari J, and Kujala UM, "Prevention of sports injuries: Systematic review of randomized controlled trials," *Arch. Intern. Med.*, vol. 167, no. 15, pp. 1585–1592, Aug. 2007.
- [18] B. L. Riemann and K. M. Guskiewicz, "Effects of Mild Head Injury on Postural Stability as Measured Through Clinical Balance Testing," *J. Athl. Train.*, vol. 35, no. 1, pp. 19–25, 2000.
- [19] C. Testerman and R. V. Griend, "Evaluation of Ankle Instability Using the Biodex Stability System," *Foot Ankle Int.*, vol. 20, no. 5, pp. 317–321, May 1999.
- [20] I.-C. Chen, P.-T. Cheng, C.-L. Chen, S.-C. Chen, C.-Y. Chung, and T.-H. Yeh, "Effects of balance training on hemiplegic stroke patients," *Chang Gung Med. J.*, vol. 25, no. 9, pp. 583–590, Sep. 2002.
- [21] Mark V. Paterno PT, MS, SCS, ATC, Greg D. Myer MS, CSCS, Kevin R. Ford MS, and Timothy E. Hewett, PhD, "Neuromuscular Training Improves Single-Limb Stability in Young Female Athletes," *J. Orthop. Sports Phys. Ther.*, vol. 34, no. 6, pp. 305–316, Jun. 2004.

- [22] R. J. Peterka, "Simplifying the complexities of maintaining balance," *IEEE Eng. Med. Biol. Mag.*, vol. 22, no. 2, pp. 63–68, 2003.
- [23] D. A. Winter, *The biomechanics and motor control of human gait: normal, elderly and pathological*. University of Waterloo Press, 1991.
- [24] James R. Chagdes, "Limit Cycle Oscillations in Standing Human Posture," *Rev.*
- [25] D. Winter, "Human balance and posture control during standing and walking," *Gait Posture*, vol. 3, no. 4, pp. 193–214, Dec. 1995.
- [26] I. J. Pinter, R. van Swigchem, A. J. K. van Soest, and L. A. Rozendaal, "The Dynamics of Postural Sway Cannot Be Captured Using a One-Segment Inverted Pendulum Model: A PCA on Segment Rotations During Unperturbed Stance," *J. Neurophysiol.*, vol. 100, no. 6, pp. 3197–3208, Dec. 2008.
- [27] Y. Aramaki, D. Nozaki, K. Masani, T. Sato, K. Nakazawa, and H. Yano, "Reciprocal angular acceleration of the ankle and hip joints during quiet standing in humans," *Exp. Brain Res.*, vol. 136, no. 4, pp. 463–473, Feb. 2001.
- [28] C. Maurer and R. J. Peterka, "A New Interpretation of Spontaneous Sway Measures Based on a Simple Model of Human Postural Control," *J. Neurophysiol.*, vol. 93, no. 1, pp. 189–200, Jan. 2005.
- [29] J. Milton, J. L. Cabrera, T. Ohira, S. Tajima, Y. Tonosaki, C. W. Eurich, and S. A. Campbell, "The time-delayed inverted pendulum: Implications for human balance control," *Chaos Interdiscip. J. Nonlinear Sci.*, vol. 19, no. 2, p. 026110, Jun. 2009.
- [30] "Fitter First Classic Wobble Board," *Health Styles Exercise Equipment*, 2013. [Online]. Available: <http://www.healthstylesexercise.com>.
- [31] "BIODEX," *Biodex Products*. [Online]. Available: www.biodex.com.
- [32] "NeuroCom Systems," *SMART Balance Master (R)*. [Online]. Available: www.onbalance.com/products/.
- [33] P. W. Jordan, "Human factors for pleasure in product use," *Appl. Ergon.*, vol. 29, no. 1, pp. 25–33, Feb. 1998.
- [34] J. G. Richards, "The measurement of human motion: A comparison of commercially available systems," *Hum. Mov. Sci.*, vol. 18, no. 5, pp. 589–602, Oct. 1999.

- [35] R. E. Mayagoitia, A. V. Nene, and P. H. Veltink, "Accelerometer and rate gyroscope measurement of kinematics: an inexpensive alternative to optical motion analysis systems," *J. Biomech.*, vol. 35, no. 4, pp. 537–542, Apr. 2002.
- [36] R. A. Clark, Y.-H. Pua, K. Fortin, C. Ritchie, K. E. Webster, L. Denehy, and A. L. Bryant, "Validity of the Microsoft Kinect for assessment of postural control," *Gait Posture*, vol. 36, no. 3, pp. 372–377, Jul. 2012.
- [37] R. Williamson and B. J. Andrews, "Detecting absolute human knee angle and angular velocity using accelerometers and rate gyroscopes," *Med. Biol. Eng. Comput.*, vol. 39, no. 3, pp. 294–302, May 2001.
- [38] A. D. Young, "From Posture to Motion: The Challenge for Real Time Wireless Inertial Motion Capture," in *Proceedings of the Fifth International Conference on Body Area Networks*, New York, NY, USA, 2010, pp. 131–137.
- [39] "Kinect for Windows Sensor Components and Specifications," *Microsoft Developer Network*. [Online]. Available: msdn.microsoft.com/en-us/library/jj131033.aspx.
- [40] "Developing Custom Measurement and Control I/O Hardware with the cRIO," *National Instruments*. [Online]. Available: www.ni.com/white-paper/3261/en.
- [41] "Tracking Users with Kinect Skeletal Tracking," *Microsoft Developer Network*. [Online]. Available: msdn.microsoft.com/en-us/library/jj131025.aspx.
- [42] R. W. Simmons, C. Richardson, and R. Pozos, "Postural stability of diabetic patients with and without cutaneous sensory deficit in the foot," *Diabetes Res. Clin. Pract.*, vol. 36, no. 3, pp. 153–160, Jun. 1997.
- [43] L. Allet, S. Armand, R. A. de Bie, A. Golay, D. Monnin, K. Aminian, J. B. Staal, and E. D. de Bruin, "The gait and balance of patients with diabetes can be improved: a randomised controlled trial," *Diabetologia*, vol. 53, no. 3, pp. 458–466, Mar. 2010.
- [44] A. A. Priplata, B. L. Prittiti, J. B. Niemi, R. Hughes, D. C. Gravelle, L. A. Lipsitz, A. Veves, J. Stein, P. Bonato, and J. J. Collins, "Noise-enhanced balance control in patients with diabetes and patients with stroke," *Ann. Neurol.*, vol. 59, no. 1, pp. 4–12, Jan. 2006.
- [45] J. G. Carbonell, R. S. Michalski, and T. M. Mitchell, "An Overview of Machine Learning," in *Machine Learning*, R. S. Michalski, J. G. Carbonell, and T. M. Mitchell, Eds. Springer Berlin Heidelberg, 1983, pp. 3–23.

APPENDIX

APPENDIX. HUMAN TESTING DOCUMENTS

Human Testing procedure

Before participant arrives:

- Calibrate the sensors
 - Line them up in the calibration position, click calibrate
 - Double check each sensor in Sensor Suite to make sure they look accurate
- Make Sure all Sensors are fully charged
- Put sensors in straps and layout in order (head, chest, hips, thigh, calf)
- Set up Kinect:
 - Physically put it in the desired location
 - Open Kinect Studio (program used to record video)

After Participant enters lab area

- Read the participant the procedure so that they know what to expect
- Let the participant stand on the board for 1 minute (record this)
- Have participant sign the consent form
- Weigh Participant
- Measure height of participant
- Attach sensors to participant
 - Sensors are attached to person at 5 spots:
 - i. Head
 - ii. Chest
 - iii. Hips
 - iv. Right thigh
 - v. Right calf
 - Make sure sensor is correctly positioned on balance board
- Make sure Kinect can see entire person and is ready to record
- Perform quick, simple test to make sure all 6 sensors are being read properly

- Give participant their instructions for the testing (see next page)
- Perform discrete step stiffness test, then a 3 minute break (x4)
- Perform linearly varying stiffness test, then a 2 minute break (x4)
- Perform time delay test, then a 2 minute break (x4)
- Remove sensors from participant
- Pay the subject and fill out the human subject receipt log
- Ask if they have any additional questions or things they need to mention

Detailed Description of Each Test

Instructions to Participant:

- Line up ankle with center line on the board. We will mark your feet in this position.
- Put on glasses to prevent you from looking down. Look straight ahead--a star sticker is on the wall to give you a focal point if needed.
- During the test, your goal is to keep the board horizontal
- Try not to grab the handrails during the test. If you do, let go as soon as possible and attempt to balance without holding on.
- If you have any general questions about the test or the balance board, please save them until after we are done testing, when we would be happy to answer any/all questions.

Discrete Step Stiffness Test

- Stiffness initially is set to its maximum value—based on the participant's height and weight
- Stiffness and damping values decrease by a constant step size (10% of maximum) every 10 seconds
- The minimum stiffness and damping values are zero, once they reach this point, they begin to increase by the same step size every 10 seconds
- When the values reach their initial values, the test ends

Linearly Varying Stiffness Test

- Stiffness initially set to its maximum value—based on the participant's height and weight
- Stiffness and damping are constantly decreased to zero—this takes about one minute
- After the values reach zero, the program automatically begins to constantly increase the values until they reach the initially values—this takes about one minute
- When the values reach their initial values, the test ends

Time Delay Test

- Stiffness is set to a value just below the stability point of the participant (75% of K^{cr})
- Stiffness and damping values stay constant throughout the test
- Time delay value initially set to zero
- Time delay increases by 50 milliseconds every 10 seconds
- Maximum time delay is 400 milliseconds
- Once value reaches maximum, it starts to decrease by 50 milliseconds every 10 seconds
- Test ends when time delay returns to zero

Naming Convention

Test Name:

SDS = stiffness, discrete step

SLR = stiffness, linear ramp

TD = time delay

Test Run:

1, 2, 3, 4

Date:

62714

Participant:

01, 02, 03

- Each File Name saved TestName_TestRun_Date_Participant
 - Example: SDS_1_62714_02
 - Discrete step stiffness test, 1st run, testing on 6/27/14, participant #2
- Folder Name: Date_Participant
 - Example: 62714_02

Summary of Timing

Introduction & Signing Consent Form: 5 minutes
 Individual Practice Time on Board: 1 minute
 Sensor Placement: 5 minutes
 Double Check everything is ready: 2 minutes
 Mark Feet: 1 minute
(Prep: 14 minutes)
 Stiffness Discrete Step Test: 3 minutes, 30 seconds
 Break: 3 minutes
 Stiffness Discrete Step Test: 3 minutes, 30 seconds
 Break: 3 minutes
 Stiffness Discrete Step Test: 3 minutes, 30 seconds
 Break: 3 minutes
 Stiffness Discrete Step Test: 3 minutes, 30 seconds
 Break: 3 minutes
(Test 1: 26 minutes)
 Stiffness Linear Ramping Test: 3 minutes, 15 seconds
 Break: 3 minutes
 Stiffness Linear Ramping Test: 3 minutes, 15 seconds
 Break: 3 minutes
 Stiffness Linear Ramping Test: 3 minutes, 15 seconds
 Break: 3 minutes
 Stiffness Linear Ramping Test: 3 minutes, 15 seconds
 Break: 3 minutes
(Test 2: 25 minutes)
 Time Delay Test: 2 minutes, 10 seconds
 Break: 2 minutes
 Time Delay Test: 2 minutes, 10 seconds
 Break: 2 minutes
 Time Delay Test: 2 minutes, 10 seconds
 Break: 2 minutes
 Time Delay Test: 2 minutes, 10 seconds
(Test 3: 14 minutes, 40 seconds)
 Remove Sensors: 2 minutes
 Answer any Questions: 5 minutes
(Wrap-Up: 7 minutes)
Total: 86 minutes, 40 seconds

VITA

VITA

Denise Cruise
Graduate School, Purdue University

Education

B.S., Biomedical Engineering, 2011, Purdue University, West Lafayette, Indiana

M.S., Mechanical Engineering, 2014, Purdue University, West Lafayette, Indiana

Research Interests

Biomechanics

Human Motion Kinetics

Human Motor Control